

IL-22 and its receptors are increased in human and experimental COPD and contribute to pathogenesis

Malcolm R. Starkey¹, Maximilian W. Plank¹, Paolo Casolari², Alberto Papi², Stelios Pavlidis³, Yike Guo³, Guy J.M. Cameron¹, Tatt Jhong Haw¹, [Anthony Tam^{4,5}](#), [Ma'en Obiedat^{4,5}](#), Chantal Donovan¹, Nicole G. Hansbro^{1,64}, Duc H. Nguyen¹, Prema Mono Nair¹, Richard Y. Kim¹, Jay C. Horvat¹, Gerard E. Kaiko¹, Scott K. Durum⁷⁵, Peter A. Wark¹, [Don D. Sin^{4,5}](#), Gaetano Caramori⁸⁶, Ian M. Adcock³, Paul S. Foster¹ and Philip M. Hansbro^{1,64}

Affiliations: ¹Priority Research Centres GrowUpWell and Healthy Lungs, School of Biomedical Sciences and Pharmacy, Hunter Medical Research Institute & University of Newcastle, Callaghan, New South Wales, Australia. ²Interdepartmental Study Center for Inflammatory and Smoke-related Airway Diseases (CEMICEF), Cardiorespiratory and Internal Medicine Section, University of Ferrara, Ferrara, Italy. ³The Airways Disease Section, National Heart & Lung Institute, Imperial College London, London, UK. ~~⁴Centre for inflammation, Centenary Institute, Sydney, and School of Life Sciences, University of Technology, Ultimo, NSW, Australia.~~ ~~⁴The University of British Columbia Center for Heart Lung Innovation, St Paul's Hospital, Vancouver, Canada.~~ ~~⁵Respiratory Division, Department of Medicine, University of British Columbia, Vancouver, BC.~~ ~~⁶Centre for inflammation, Centenary Institute, Sydney, and School of Life Sciences, University of Technology, Ultimo, NSW, Australia.~~ ⁷⁵Laboratory of Immunoregulation, Cancer and Inflammation Program, Center for Cancer Research, National Cancer Institute, National Institutes of Health, Frederick, MD, USA. ⁸⁶UOC di Pneumologia, Dipartimento di Scienze Biomediche,

1
2
3 25 Odontoiatriche e delle Immagini Morfologiche e Funzionali (BIOMORF), Università di
4
5 26 Messina, Italy.

7
8 27 **Correspondence:** Professor Philip M. Hansbro, Centre for inflammation, Centenary
9
10 28 Institute, Sydney, and School of Life Sciences, University of Technology, Ultimo,
11
12 29 NSW, Australia. E-mail: p.hansbro@centenary.org.au

14
15 30 **Take home message**

16
17 31 IL-22 and its receptors are increased in both human and experimental COPD. IL-22
18
19 32 drives neutrophilic inflammation and impaired lung function in experimental chronic
20
21 33 obstructive pulmonary disease (195 characters)

23
24 34
25
26 35 This article has supplementary material available from erj.ersjournals.com

27
28 36
29
30
31 37 Support statement: The National Health and Medical Research Council of Australia,
32
33 38 Australian Research Council, The University of Newcastle and Hunter Medical
34
35 39 Research Institute

36
37 40
38
39
40 41 Funding information for this article has been deposited with FundRef.

41
42 42
43
44 43 Conflict of interest: Disclosures can be found alongside the online version of this
45
46 44 article at erj.resjournals.com

1
2
3
4 45 **ABSTRACT** Chronic Obstructive Pulmonary Disease (COPD) is the third leading
5
6 46 cause of morbidity and death globally. The lack of effective treatments results from
7
8 47 an incomplete understanding of the underlying mechanisms driving COPD
9
10
11 48 pathogenesis.

12
13 49 Interleukin (IL)-22 has been implicated in airway inflammation and is increased in
14
15 50 COPD patients. However, its roles in the pathogenesis of COPD is poorly
16
17 51 understood. Here, we investigated the role of IL-22 in human COPD and in cigarette
18
19 52 smoke (CS)-induced experimental COPD.

20
21
22 53 IL-22 and IL-22 receptor mRNA expression and protein levels were increased in
23
24 54 COPD patients compared to healthy smoking or non-smoking controls. IL-22 and IL-
25
26 55 22 receptor levels were increased in the lungs of mice with experimental COPD
27
28 56 compared to controls and the cellular source of IL-22 included CD4⁺ T-helper cells,
29
30 57 $\gamma\delta$ T-cells, Natural Killer T-cells and group 3 innate lymphoid cells. CS-induced
31
32 58 pulmonary neutrophils were reduced in IL-22-deficient (*IL22^{-/-}*) mice. CS-induced
33
34 59 airway remodelling and emphysema-like alveolar enlargement did not occur in *IL22^{-/-}*
35
36 60 mice. *IL22^{-/-}* mice also had improved lung function in terms of airway resistance, total
37
38 61 lung capacity, inspiratory capacity, forced vital capacity and compliance.

39
40
41 62 These data highlight important roles for IL-22 and its receptors in human COPD and
42
43 63 CS-induced experimental COPD.

44
45
46 64 **Max number of words: 200 (current: 195 words)**
47
48
49
50
51
52
53
54
55
56
57
58
59
60

66 Introduction

67 Chronic Obstructive Pulmonary Disease (COPD) is the third leading cause of
68 morbidity and death and imposes a significant socioeconomic burden globally [1]. It
69 is a complex, heterogeneous disease characterised by chronic pulmonary
70 inflammation, airway remodelling and emphysema, which are associated with
71 progressive lung function decline [2]. Cigarette smoke (CS) is a major risk factor for
72 COPD [2]. The mainstay therapies for COPD are glucocorticoids, β_2 -adrenergic
73 receptor agonists and long-acting muscarinic antagonists [3]. However, these agents
74 only provide symptomatic relief rather than modifying the causal factors or
75 suppressing disease progression [3]. There is emerging interest in altered lung and
76 gut microbiomes and the gut-lung axis that could be modified for therapeutic gain [4,
77 5]. Nevertheless, there is currently a lack of effective treatments for COPD due to the
78 poor understanding of the underlying mechanisms.

79 Interleukin (IL)-22 is a member of the IL-10 cytokine family that is implicated in
80 several human diseases, including mucosal-associated infections and inflammatory
81 disorders of the lung [6]. CD4⁺ T-helper cells, $\gamma\delta$ T-cells, natural killer T (NKT)-cells
82 and group 3 innate lymphoid cells (ILC3) are generally the major cellular sources of
83 IL-22 [6]. Unlike IL-22, expression of the IL-22 receptor (IL-22R) is largely restricted
84 to structural cells. This ligand-receptor distribution permits immune cells to regulate
85 responses of stromal cells and particularly at barrier surfaces such as the lung,
86 where epithelial cells play an active role in initiating, regulating, and resolving
87 immune responses. IL-22R is a cell surface heterodimer consisting of IL-22RA1 and
88 IL-10RB [6]. IL-22RA2 is a naturally occurring IL-22 antagonist that negatively
89 regulates IL-22-induced inflammatory responses [6, 7]. Functional studies in murine
90 systems indicate that IL-22 has immune-regulatory properties in infection,

1
2
3 91 inflammation, autoimmunity, and cancer [6]. In these models, the functional
4
5 92 consequences of IL-22 expression can be either pathologic or protective, depending
6
7
8 93 on the context in which it is expressed. Indeed, increased IL-22 levels and IL-22⁺
9
10 94 cells have been demonstrated in the blood, sputum and lung biopsies of COPD
11
12 95 patients [8]. The role of IL-22 in lung antimicrobial defence and the impact of COPD
13
14 96 on this defence pathway has been reported [9, 10]. In experimental COPD
15
16 97 *Haemophilus influenzae* infection impaired IL-22 production and wild-type and IL-22-
17
18 98 deficient (^{-/-}) mice had impaired clearance [10]. CS exposure suppressed
19
20
21 99 *Streptococcus pneumoniae* induced IL-22 production and treatment with
22
23
24 100 recombinant IL-22 restored bacterial clearance [11]. Despite this, there is limited
25
26 101 knowledge of the role IL-22 plays in COPD pathogenesis independent of respiratory
27
28
29 102 infection.

30
31 103 Here, we investigate its role using gene expression analysis of airway
32
33 104 epithelial brushings and parenchymal cores from human COPD patients, an
34
35 105 established mouse model of CS-induced experimental COPD that recapitulates the
36
37 106 critical features of human disease [4, 12-18], and IL-22 reporter and *IL22*^{-/-} mice [19].
38
39 107 IL-22 and IL-22R mRNA and protein were increased in the airways of mild-moderate
40
41
42 108 COPD patients. IL-22 and IL-22⁺ T-cells and ILC3s were increased in experimental
43
44 109 COPD. CS-induced pulmonary neutrophilic inflammation, airway remodelling and
45
46 110 emphysema were reduced and lung function was improved in *IL22*^{-/-} mice compared
47
48
49 111 to WT controls, thus implicating IL-22 in COPD pathogenesis.
50

51
52 112

53 54 55 113 **Methods**

56
57 114 Ethics statement, animal details, additional methods and statistical analyses are
58
59
60 115 described in online supplementary material.

116

117 **Human gene expression.** Analysis of IL22, IL22RA1, IL10RB and IL22RA2 in
118 published human array datasets (Accession numbers: GSE5058 and GSE27597)
119 [20-22] was performed using Array Studio software (Omicsoft Corporation, Research
120 Triangle Park, NC, USA).

121

122 **Mice.** Female, 7-8-week-old, WT C57BL/6 mice, *Il17a^{eGFP/+};Il22^{td-tomato/+}* reporter and
123 *Il22^{-/-}* mice on a C57BL/6 background [19].

124

125 **Experimental COPD.** Mice were exposed to normal air or nose-only inhalation of CS
126 for eight weeks in a protocol representative of a pack-a-day smoker as extensively
127 described previously [4, 12-18, 23, 24].

128

129 **qPCR.** Total RNA was extracted from whole lung tissue and blunt-dissected airways
130 and parenchyma and reversed transcribed [13]. mRNA transcripts were determined
131 by real-time quantitative PCR (qPCR, ABIPrism7000, Applied Biosystems, Scoresby,
132 Victoria, Australia) using custom designed primers (Integrated DNA Technologies,
133 Baulkham Hills, New South Wales, Australia) (**supplementary table 1**).

134

135 **Flow Cytometry.** IL-17A⁺ and IL-22⁺ CD4⁺ T-cells, $\gamma\delta$ T-cells, NKT-cells and ILC3s
136 in lung homogenates were determined based on surface marker expression
137 (**supplementary table 2**) [25-27] using a BD FACSAriaIII. Flow cytometry antibodies
138 were from Biolegend (Karrinyup, Australia) or BD Biosciences (North Ryde,
139 Australia) (**supplementary table 3, supplementary figure 1**).

140

1
2
3 141 **Pulmonary Inflammation.** Airway inflammation was assessed by differential
4
5 142 enumeration of inflammatory cells in bronchoalveolar lavage fluid (BALF) [12, 14, 28,
6
7 143 29]. BALF supernatants were stored at -20°C for assessment of IL-22 protein levels.
8
9 144 Tissue inflammation was assessed by enumeration of inflammatory cells [12-14, 29]
10
11
12 145 and histopathological scoring based on established criteria [30].
13
14
15 146

16
17 147 **ELISA.** IL-17A, IL-22, MPO and neutrophil elastase protein levels were quantified
18
19 148 with commercially available ELISA kits (R&D Systems or Biolegend) [19].
20
21
22 149

23
24 150 **Immunohistochemistry (IHC).** Lungs were perfused, inflated, formalin fixed,
25
26 151 paraffin embedded, and sectioned (4µm)[13, 14]. Longitudinal sections of the left
27
28 152 lung were deparaffinized and stained with antibodies against IL-22R~~Aa~~1 or IL-
29
30 153 22R~~Aa~~2. IHC in human samples is described in online supplement (supplementary
31
32
33 154 tables 4-65)[31].
34
35
36 155

37
38 156 **Airway Remodelling.** Airway epithelial (µm²) and collagen deposition area (µm²)
39
40 157 were assessed in a minimum of four small airways (basement membrane [BM]
41
42 158 perimeter <1,000µm) per section [12-14, 17, 18]. Data were quantified using ImageJ
43
44 159 software (Version 1.50, NIH) and normalised to BM perimeter (µm).
45
46
47 160

48
49 161 **Alveolar Enlargement.** Alveolar diameter was assessed using the mean linear
50
51 162 intercept technique [12-14, 17, 18, 32].
52
53
54 163

55
56 164 **Lung Function.** Mice were anaesthetised with ketamine (100mg/kg) and xylazine
57
58 165 (10mg/kg), tracheas cannulated and attached to Buxco® Forced Manoeuvres
59
60

1
2
3 166 apparatus (DSI, St. Paul, Minnesota, USA) to assess total lung capacity (TLC) [12,
4
5 167 13]. FlexiVent apparatus (FX1 System; SCIREQ, Montreal, Canada) was used to
6
7
8 168 assess lung volume, airway resistance, inspiratory capacity (IC), forced vital capacity
9
10 169 (FVC), compliance and elastance (tidal volume: 8mL/kg, respiratory rate: 450
11
12 170 breaths/min) [12, 33, 34].
13
14
15 171

172 **Results**

173 **IL-22 and IL-22R mRNA expression and protein levels are increased** 174 **in human COPD**

175 We first determined whether the mRNA expression of IL-22, and its receptors IL-
176 22RA1 and IL-10RB and antagonist IL-22RA2 were altered in humans with mild-to-
177 moderate COPD (GOLD Stage I or II Accession: GSE5058 [20, 21, 35]). Pre-existing
178 microarray data from airway epithelial brushings of healthy non-smokers, healthy
179 smokers and COPD patients were interrogated [20]). IL22, IL22RA1, IL10RB and
180 IL22RA2 mRNA expression were not significantly altered in airway epithelial
181 brushings from healthy smokers compared to non-smokers (**Figure 1a-d**).
182 Importantly, however, IL22 (2.01-fold), IL22RA1 (2.48-fold), IL10RB (3.26-fold) and
183 IL22RA2 (1.78-fold) mRNA expression were increased in airway epithelial brushings
184 from patients with mild-to-moderate COPD compared to non-smokers. Similar results
185 were observed when mild-to-moderate COPD was compared to healthy smokers.

186 We then assessed the mRNA expression of IL-22 and its receptors in pre-
187 existing microarray data from lung parenchyma cores from severe COPD patients
188 (GOLD Stage IV [35] Accession: GSE27597 [22]). There was no change in IL22,
189 IL22RA1, IL10RB or IL22RA2 expression in cores from COPD patients compared to
190

1
2
3 190 non-smokers without COPD (**Figure 1e-h**). IL-22, IL-22RA1, IL-22RA2 and IL-10RB
4
5 191 were unchanged in peripheral lung tissue from patients with mild emphysema
6
7 192 (supplementary figure 2 from GSE8581). There was no significant correlation
8
9
10 193 between pack years and IL-22, IL-22RA1 and IL-22RA2 gene expression in lung
11
12 194 tissue (supplementary figure 3 from GSE17770). Using lung cancer as a disease
13
14 195 control, no differential expression of IL-22, IL-22RA1, IL-22RA2 or IL-10RB in either
15
16 196 bronchial brushings (GSE4115) or lung tissue (GSE1650) between healthy smokers
17
18 197 and subjects with lung cancer were observed (**supplementary figures 4-5**).

19 20
21 198 Finally, we assessed IL-22 and receptor protein levels in human COPD by
22
23 199 IHC. The percentage of IL-22⁺ alveolar macrophages and IL-22RA1⁺ and IL-10RB⁺
24
25 200 airway epithelial cells were increased in COPD compared to age- and smoke history-
26
27 201 matched smokers with normal lung function (**Figure 2, supplementary figure 6** and
28
29 202 supplementary tables 6-9). No change in IL-22RA2 was detected (supplementary
30
31 203 table 8).

32
33
34
35 204 In a separate cohort of COPD patients, IL-22RA1 was also increased in
36
37 205 airway epithelial cells of current smokers with COPD compared to non-smokers
38
39 206 (Supplementary Figure 7 and supplementary table 10). When combined with ex-
40
41 207 smokers with COPD, these IL-22RA1 signal in the airway epithelium is lost
42
43 208 (Supplementary Figure 7).
44
45
46
47 209

48 49 210 **IL-22 and receptor protein levels are increased in the lungs in** 50 51 **experimental COPD**

52 211 We next investigated the expression of IL-22 and its receptors in CS-induced
53
54 212 experimental COPD, which models mild-to-moderate COPD. We first confirmed that
55
56 213 IL-22 was increased in experimental COPD. *IL22* mRNA was difficult to detect in
57
58 214
59
60

1
2
3 215 mouse lungs, therefore we assessed protein levels by ELISA in both whole lung
4
5 216 homogenates (includes both airways and parenchyma) and BALF supernatants. CS-
6
7 217 exposure of WT mice resulted in increased IL-22 protein levels in lung homogenates,
8
9 218 but not BALF supernatants compared to normal air-exposed controls (**figure 3a-b**).
10
11 219 IL-22 protein levels were unaltered following 1 week of CS exposure
12
13 220 (**supplementary figure 87**). Collectively, these data show that IL-22 is increased in
14
15 221 both human and experimental COPD and are consistent with previous reports [8].
16
17
18

19 222 Next, we assessed IL-22 receptor expression in blunt-dissected airways
20
21 223 *versus* parenchymal tissue [13]. CS-exposure had no statistically significant effect on
22
23 224 *Il22ra1* or *Il10rb* mRNA expression, but did reduce *Il22ra2* expression in the airways
24
25 225 compared to normal air-exposed controls (**figure 3c-e**). CS exposure also did not
26
27 226 affect *Il22ra1* or *Il22ra2* mRNA expression, but did increase *Il10rb* expression in the
28
29 227 parenchyma compared to normal air-exposed controls (**figure 3f-h**). Whilst no
30
31 228 statistically significant differences in *Il22ra1* mRNA expression were observed in this
32
33 229 model, it is notable that *Il22ra1* mRNA expression was ~10-fold higher in the airways
34
35 230 than the parenchyma.
36
37
38

39 231 Finally, we assessed IL-22 receptor protein expression in mouse lung tissue
40
41 232 sections. CS-exposure resulted in notable increases in both IL-22RA1 and IL-22RA2
42
43 233 protein levels, particularly in airway epithelial cells but also alveolar macrophages
44
45 234 (**supplementary figure 98**).
46
47
48

49 235

50 51 236 **IL-22⁺ CD4⁺ T-cells, $\gamma\delta$ T-cells, NKT-cells and ILC3s are increased in** 52 53 54 237 **the lungs in experimental COPD**

55
56
57 238 Given that IL-22 is increased in both human and experimental COPD, we next
58
59 239 defined the cellular source of increased pulmonary IL-22 using *Il17a^{eGFP/+};Il22^{td-}*

1
2
3 240 *tomato*⁺ reporter mice that enable the detection of IL-17A⁺ and IL-22⁺ cells without ex
4
5 241 *vivo* stimulation. CS-exposure of reporter mice resulted in increased numbers of IL-
6
7 242 17A⁺, IL-22⁺ and IL-17A⁺IL-22⁺ CD4⁺ T-cells, $\gamma\delta$ T-cells, NKT-cells and ILC3s
8
9 243 compared to normal air-exposed controls (**figure 4a-p**). We then assessed the
10 244 relative proportions of these cells following CS-exposure (**figure 4q-s**). As previously
11 245 shown [36], $\gamma\delta$ T-cells were the dominant source of IL-17A following CS exposure
12 246 (**figure 4q**). CD4⁺ T-cells, NKT-cells, and ILC3s were the major IL-22-producing cells
13 247 (**figure 4r**), whilst NKT-cells were the dominant source of dual IL-17A⁺IL-22⁺ cells
14 248 (**figure 4s**).

249

250 **CS-induced pulmonary neutrophils were reduced in *Il22*^{-/-} mice**

251 We next investigated whether IL-22 plays a role in the pathogenesis of experimental
252 COPD. WT and *Il22*^{-/-} mice were exposed to normal air or CS for 8 weeks [12-18].
253 Pulmonary inflammation in BALF was assessed by staining and differential
254 enumeration of inflammatory cells. CS exposure of WT mice resulted in significantly
255 increased total leukocytes, macrophages, neutrophils and lymphocytes compared to
256 normal air-exposed WT controls (**figure 5a-d**). CS-exposed *Il22*^{-/-} mice also had
257 increased numbers of these cells compared to normal air-exposed *Il22*^{-/-} controls.
258 Neutrophils were significantly reduced, but total leukocytes, macrophages and
259 lymphocytes were unaltered in CS-exposed *Il22*^{-/-} mice compared to CS-exposed
260 WT controls.

261 We then assessed inflammatory cell numbers in lung tissue sections [12-14,
262 29]. CS exposure of WT mice significantly increased inflammatory cell numbers in
263 the parenchyma compared to normal air-exposed WT controls (**figure 5e-f**). CS-
264 exposed *Il22*^{-/-} mice also had increased parenchymal inflammatory cells compared to

1
2
3 265 their normal air-exposed controls. Numbers of parenchymal inflammatory cells were
4
5 266 not different between CS-exposed *Il22^{-/-}* and WT mice.
6
7

8 267 Next, histopathology was scored according to a set of custom-designed
9
10 268 criteria as described previously [30]. CS exposure of WT mice increased
11
12 269 histopathology score, which was characterised by increased airway, vascular and
13
14 270 parenchymal inflammation (**figure 5g-k**). CS-exposed *Il22^{-/-}* mice also had increased
15
16 271 histopathology, airway, vascular and parenchymal inflammation scores compared to
17
18 272 their normal air-exposed controls. *Il22^{-/-}* mice had a small but significant reduction in
19
20 273 total histopathology score, compared to CS-exposed WT controls.
21
22
23

24 274 We then profiled the mRNA expression of chemokines and cytokines, other
25
26 275 than IL-22, that are involved in neutrophil influx into the lung including chemokine (C-
27
28 276 X-C motif) ligand (CXCL)1, CXCL2 and IL-17A [37]. CS-exposure of WT mice
29
30 277 resulted in significantly increased *Cxcl1*, *Cxcl2* and *Il17a* mRNA expression
31
32 278 compared to normal air-exposed WT controls with *Cxcl1* and *Cxcl2* having
33
34 279 approximately 200-fold greater expression than *Il17a* (**figure 5l-n**). CS-exposed *Il22^{-/-}*
35
36 280 *-/-* mice also had increased expression of *Cxcl1* and *Il17a*, but not *Cxcl2* compared to
37
38 281 normal air-exposed *Il22^{-/-}* controls. There was a significant reduction in *Cxcl2*, but not
39
40 282 *Cxcl1* or *Il17a* mRNA expression in CS-exposed *Il22^{-/-}* mice compared to CS-
41
42 283 exposed WT controls. Protein levels of IL-17A, MPO and neutrophil elastase were
43
44 284 increased in CS-exposed WT mice, but were unaltered in *Il22^{-/-}* mice
45
46 285 (**supplementary figure 109**).
47
48
49
50
51
52

53
54 287 **CS-induced increases in airway epithelial area, collagen deposition**
55
56 288 **and emphysema-like alveolar enlargement do not occur in *Il22^{-/-}***
57
58 289 **mice**
59
60

1
2
3 290 We have previously shown that CS-exposed WT mice develop small airway
4
5 291 remodelling (increased epithelial area), fibrosis (collagen deposition) and
6
7 292 emphysema-like alveolar enlargement after 8 weeks of CS exposure [12-14, 17, 18,
8
9 293 32]. Thus, we next determined whether IL-22 contributes to these disease features.
10
11
12 294 In agreement with our previous studies, CS exposure of WT mice increased small
13
14 295 airway epithelial cell area compared to normal air-exposed WT controls (**figure 6a-**
15
16 296 **b**). In contrast, CS-exposed *IL22^{-/-}* mice had no change in airway epithelial cell area
17
18
19 297 compared to normal air-exposed *IL22^{-/-}* controls.

20
21 298 CS-exposed WT mice had increased collagen deposition compared to normal
22
23 299 air-exposed WT controls (**figure 6c-d**). However, CS-exposed *IL22^{-/-}* mice did not
24
25 300 have increased collagen deposition compared to *IL22^{-/-}* normal air-exposed controls.

26
27 301 CS-exposed WT mice had significantly increased alveolar diameter compared
28
29 302 to normal air-exposed WT controls (**figure 6e-f**). CS-exposed *IL22^{-/-}* mice did not
30
31 303 have increased alveolar diameter compared normal air-exposed *IL22^{-/-}* controls.

32
33 304 As a result of the relatively small differences in airway epithelial area, collagen
34
35 305 deposition and alveolar diameter the differences were not statistically different
36
37 306 between CS-exposed *IL22^{-/-}* mice and CS-exposed WT controls.

38
39
40
41
42 307

43 44 308 **CS-induced lung function impairment is improved in *IL22^{-/-}* mice**

45
46 309 We next assessed the role of IL-22 in CS-induced impairment of lung function,
47
48 310 measured in terms of lung volume, airway resistance, TLC, IC, FVC and compliance.

49
50 311 CS-exposed WT mice had increases in all of these parameters compared to normal
51
52 312 air-exposed WT controls (**Figure 7a-f**). In CS-exposed *IL22^{-/-}* mice none of these lung
53
54 313 function parameters were significantly different compared to normal air-exposed *IL22^{-/-}*
55
56 314 *-/-* controls. Again, likely due to small changes in mild-moderate experimental COPD,
57
58
59
60

1
2
3 315 these lung function parameters were not significantly altered in CS-exposed *Il22*^{-/-}
4
5 316 mice compared to CS-exposed WT controls. However, CS-exposed *Il22*^{-/-} mice had
6
7 317 similar lung function to air-exposed WT controls.
8
9

10 318 We also assessed tissue elastance and found a non-significant reduction in
11
12 319 CS-exposed WT mice that was not different in *Il22*^{-/-} mice (**supplementary figure**
13
14
15 320 **110**).
16

17 321 Discussion

18
19
20 322 Here, we demonstrate that IL-22 plays a previously undefined role in the
21
22 323 pathogenesis of CS-induced experimental COPD. IL-22 and its receptors were
23
24 324 increased in both human and experimental COPD. We show for the first-time using
25
26 325 IL-22 reporter mice, that elevated lung IL-22 levels in experimental COPD result from
27
28 326 increased IL-22⁺ CD4⁺ T-cells, $\gamma\delta$ T-cells, NKT-cells and ILC3s. We also
29
30 327 demonstrated that CS-induced neutrophilic airway inflammation, was reduced in *Il22*^{-/-}
31
32 328 ^{-/-} mice compared to WT controls. Furthermore, *Il22*^{-/-} mice did not develop CS-
33
34 329 induced airway remodelling and emphysema and had improved lung function that
35
36 330 was comparable to normal air-exposed controls. Hence, this study provides new
37
38 331 insights into the roles of IL-22 in the pathogenesis of COPD.
39
40
41
42

43 332 The presence or absence of IL-22 may affect resident microbiota. Indeed, we
44
45 333 have reviewed the pathogenic roles for gut and lung microbiota in the development
46
47 334 of COPD [5, 38, 39]. To minimise the influence of altered microbiota WT and *Il22*^{-/-}
48
49 335 mice were derived from the same breeding pairs, maintained in the same facility and
50
51 336 used experimentally at the same time, and so they would be expected to have very
52
53 337 similar microbiomes.
54
55
56

57 338 Using pre-existing microarray datasets, we show that IL-22 and IL-22R mRNA
58
59 339 expression were increased in airway epithelial cells from patients with mild-to-
60

1
2
3 340 moderate COPD [20]. However, IL-22 and IL-22R mRNA were unaltered in lung
4
5 341 parenchymal cores in severe COPD [22]. Our data are supported by studies that
6
7 342 show increased IL-22 protein levels and IL-22⁺ immune cells in blood, sputum and
8
9 343 lung biopsies of COPD patients (reviewed in [8]). However, there are limited reports
10
11 344 of IL-22 receptor expression in COPD. Neutrophil proteases have been shown alter
12
13 345 IL-22R-dependent antimicrobial defence in COPD but there was no change in
14
15 346 IL22RA1 mRNA expression in lung tissue or primary cultures of proximal airway
16
17 347 epithelial cells from COPD patients compared to healthy controls [9]. IL-10RB and IL-
18
19 348 22RA2 have not been assessed in COPD. Consistent with our human data, IL-22
20
21 349 was also increased in lung tissue homogenates in experimental COPD after 8 weeks
22
23 350 but not before the development of disease upon 1 week of CS exposure. IL-22
24
25 351 receptor mRNA expression was different between human and mouse. However, at
26
27 352 the protein level, IL-22RA1 and RA2 were visually increased in the airway epithelium
28
29 353 of CS-exposed mice, which was consistent with changes at the mRNA level in
30
31 354 humans. IL-22 receptors were also increased at protein level in human COPD.
32
33 355 Collectively, our data show that IL-22 and its receptors are increased in both human
34
35 356 and experimental COPD. However, the expression of IL-22 and its receptors is
36
37 357 heterogenous and is influenced by tissue location and disease severity.

38
39
40 358 Given that IL-22 was increased in the lungs in experimental COPD, we
41
42 359 utilised IL-17A and IL-22 dual reporter mice that facilitate the identification of IL-17A-
43
44 360 and IL-22-expressing immune cells without *ex vivo* stimulation or cell fixation. This
45
46 361 enables a more accurate determination of the *in vivo* lung environment. We show for
47
48 362 the first time that CS exposure induced IL-22 production from CD4⁺ T-cells, $\gamma\delta$ T-
49
50 363 cells, NKT-cells and ILC3s, which are the major cellular sources of IL-22 and all
51
52 364 these cell subsets have known roles in COPD pathogenesis [36, 40, 41]. However,
53
54
55
56
57
58
59
60

1
2
3 365 the individual contribution of each of these cells to IL-22 production and COPD
4
5 366 pathogenesis, especially in humans remains to be fully elucidated.

7
8 367 Previously, the role of IL-22 in the pathogenesis of COPD was largely
9
10 368 unknown. We addressed this gap in knowledge using an established mouse model
11
12 369 of tightly controlled chronic nose-only CS-induced experimental COPD [12-18]. Our
13
14 370 models are representative of a pack-a-day smoker [24]. We have consistently shown
15
16 371 that 8 weeks of CS exposure in our models is sufficient to induce the hallmark
17
18 372 features of human COPD: chronic inflammation, airway remodelling, emphysema
19
20 373 and impaired lung function [12-18]. This 8-week time point was specifically chosen to
21
22 374 investigate the underlying pathogenic mechanism(s) during the early stages (GOLD
23
24 375 I/II) and identify potential therapeutic targets to halt the progression of COPD.

26
27 376 Using this established model, we show for the first time that IL-22 contributes
28
29 377 to COPD pathogenesis independently of infectious exacerbations. *Il22^{-/-}* mice had
30
31 378 reduced airway neutrophils, which was associated with decreased in *Cxcl2* mRNA
32
33 379 expression. CXCL1 and CXCL2 are the mouse orthologues/homologues of human
34
35 380 IL-8 and have critical roles in neutrophil influx into the airways following CS-exposure
36
37 381 [42]. It has been suggested that improper activation of neutrophils lies at the core of
38
39 382 COPD pathology, and mechanisms regulating their function are potential therapeutic
40
41 383 targets [43]. However, *Il22^{-/-}* mice were protected from the increases in MPO or
42
43 384 neutrophil elastase levels. *Il22^{-/-}* mice also had decreased lung tissue inflammation
44
45 385 indicated by reduced histopathological score. This is consistent with a previous
46
47 386 report showing that administration of recombinant IL-22 (rIL-22) into the lung
48
49 387 increased tissue inflammation [44].

50
51 388 We also demonstrate, as we have shown previously, that increases in airway
52
53 389 epithelial area, collagen deposition around small airways and emphysema-like
54
55
56
57
58
59
60

1
2
3 390 alveolar enlargement occur following chronic CS-exposure in WT mice [12-18].
4
5 391 Notably, these features did not develop in *IL22*^{-/-} mice compared to normal air-
6
7 392 exposed *IL22*^{-/-} controls, although the changes were not significant between CS-
8
9 393 exposed *IL22*^{-/-} mice and CS-exposed WT controls. IL-22 is essential for lung
10
11 394 epithelial cell repair following influenza virus infection and is implicated in renal
12
13 395 fibrosis [45, 46]. Others have shown that mice lacking IL-22 have delayed bacterial
14
15 396 clearance and increased alveolar wall thickening and airway remodelling [10].
16
17 397 Administration of rIL-22 with or without acute CS-exposure induced airway epithelial
18
19 398 thickening and collagen deposition, although this was not quantified [44].
20
21
22
23

24 399 Our study is the first report on the role of IL-22 in regulating multiple lung
25
26 400 function parameters, particularly in models of COPD. We show that *IL22*^{-/-} mice have
27
28 401 improved lung function in terms of lung volumes, airway resistance, TLC, IC, FVC
29
30 402 and compliance that are comparable to normal air-exposed WT mice. One previous
31
32 403 report in an acute CS-exposure model showed increased airway resistance following
33
34 404 administration of rIL-22 [44], however ours is the first study to assess lung function in
35
36 405 *IL22*^{-/-} mice.
37
38
39

40 406 The absence of IL-22 in CS-exposed *IL22*^{-/-} mice suppressed both airway
41
42 407 remodelling and concomitantly the impairment of lung function in experimental
43
44 408 COPD. Indeed CS-exposed *IL22*^{-/-} mice were protected against increases in epithelial
45
46 409 area, collagen deposition and emphysema compared to normal air-exposed controls.
47
48 410 Airway remodelling involving epithelial hyperplasia and fibrosis are important in
49
50 411 driving resistance to airflow [17, 18]. Emphysema leads to apparent increases in total
51
52 412 lung and inspiratory capacity and tissue compliance, which results from the loss of
53
54 413 alveolar and parenchymal tissue. In line with the protection against airway
55
56 414 remodelling and emphysema-like alveolar enlargement, CS-exposed *IL22*^{-/-} mice
57
58
59
60

1
2
3 415 were also protected from impaired lung function and changes in airway
4
5 416 resistance, total lung and inspiratory capacity and tissue compliance.
6
7

8 417 In summary, our study demonstrates previously unrecognised roles for IL-22
9
10 418 in COPD pathogenesis. It highlights the potential role of IL-22 in chronic lung
11
12 419 diseases, which may be a useful biomarker in the diagnosis and/or prognosis of
13
14 420 COPD patients. Furthermore, using a clinically-relevant and established model of
15
16 421 experimental COPD, our study demonstrates that IL-22 promotes CS-induced
17
18 422 pulmonary neutrophilic inflammation, airway remodelling and lung function
19
20 423 impairment. However, inhibiting IL-22 may increase the risk of exacerbations due to
21
22 424 its central role in pathogen clearance. Therefore, caution in therapeutic approaches
23
24 425 targeting IL-22 signalling are required. The relationships between IL-22 and genetic
25
26 426 factors, infections/colonisation and phenotypes in COPD remain to be defined.
27
28
29
30

31 427

32
33 428 **Max number of words: 3,000 (current 3,57023)**
34
35

36 429

37 38 39 430 **Acknowledgements**

40
41 431 This study was supported by grants from the National Health and Medical Research
42
43 432 Council (NHMRC) of Australia and the Australian Research Council (ARC). M.R.S
44
45 433 was supported by an NHMRC Early Career Research Fellowship and is supported
46
47 434 by an Australian Research Council (ARC) Discovery Early Career Researcher Award
48
49 435 (DECRA) fellowship. C.D. is supported by an NHMRC Early Career Research
50
51 436 Fellowship I.M.A is supported by Wellcome Trust grant. P.M.H is supported by an
52
53 437 NHMRC Principal Research Fellowship (1079187) and by a Brawn Fellowship,
54
55 438 Faculty of Health & Medicine, the University of Newcastle. We acknowledge Prof.
56
57 439 Dale Godfrey, The University of Melbourne for α GalCer tetramers, Kristy Wheeldon
58
59
60

1
2
3 440 and Nathalie Kiaos for CS exposure of mice, Tegan Moore for assistance with data
4
5 441 generation and Jessica Weaver for assistance with *Il22^{-/-}* and reporter mouse
6
7 442 colonies.
8
9

10 443

13 444 **Conflict of interest**

16 445 PMH reports funding/consultancies from Pharmaxis, AstraZeneca, Sanofi,
17
18 446 Pharmakea, Ausbio, and Allakos outside the submitted work. Other authors declared
19
20 447 no conflict of interest, financial or otherwise.
21
22

23 448

26 449 **Figure 1: IL-22 and IL-22R mRNA expression are increased in airway epithelial**
27
28 450 **brushings from mild-moderate human COPD patients compared to healthy**
29
30 451 **smokers and non-smokers.** Microarray data from airway epithelial cells from
31
32 452 healthy human non-smokers (NS), healthy smokers without COPD (Smoker) and
33
34 453 COPD patients with Global Initiative for Chronic Obstructive Lung Disease (GOLD)
35
36 454 stage I (Mild) or II (Moderate) disease (Accession: GSE5058 [20]) were interrogated.
37
38 455 **(a) IL22 (b) IL22RA1, (c) IL10RB, (d) IL22RA2** mRNA expression. Microarray data
39
40 456 from lung parenchymal cores from human healthy non-smokers (NS) and COPD
41
42 457 patients with GOLD) stage IV (severe) disease (Accession: GSE27597 [22]) were
43
44 458 interrogated. **(e) IL22 (f) IL22RA1, (g) IL10RB, (h) IL22RA2** mRNA expression. Data
45
46 459 are expressed as \log_2 intensity robust multi-array average signals. The Benjamini–
47
48 460 Hochberg method for adjusted P value/false discovery rate (FDR) was used to
49
50 461 analyse differences between NS, Smokers and COPD patients. * = $p < 0.005$
51
52 462 compared to COPD. ns = not significant.
53
54
55
56
57
58
59 463
60

1
2
3 464

4
5 465 **Figure 2: IL-22, IL-22RA1 and IL-10Rb, but not IL-22RA2 protein is increased in**
6 **human COPD.** IHC for IL-22 and its receptors in peripheral lung from smokers with
7
8 466 mild-to-moderate stable COPD and compared to age- and smoke history-matched
9
10 467 smokers with normal lung function. (a) IL-22⁺ alveolar macrophages, (b) IL-22RA1⁺
11
12 468 alveolar macrophages, (c) IL-22RA1⁺ airway epithelial cells, (d) IL-10RB⁺ alveolar
13
14 469 macrophages, (e) IL-10RB⁺ airway epithelial cells. Data are presented as mean \pm
15
16 470 SEM, n = 12.
17
18
19
20
21

22 472

23
24 473 **Figure 3: IL-22 protein levels are increased in the lungs of CS-exposed mice**
25 **with experimental COPD.** Wild-type (WT) C57BL/6 mice were exposed to normal
26
27 474 air or CS for 8 weeks. IL-22 protein levels in (a) lung homogenates and (b)
28
29 475 bronchoalveolar lavage fluid (BALF) supernatants were assessed by ELISA. In
30
31 476 separate experiments, airways and parenchyma were blunt-dissected and IL-22
32
33 477 receptor mRNA expression assessed. Airway (c) *Il22ra1*, (d) *Il10rb*, (e) *Il22ra2* and
34
35 478 parenchymal (f) *Il22ra1*, (g) *Il10rb* and (h) *Il22ra2* mRNA expression. Data are
36
37 479 presented as mean \pm SEM, n = 6, with another independent experiment showing
38
39 480 similar results. Two-tailed Mann-Whitney t-test was used to analyse differences
40
41 481 between two groups, whereby * = p<0.05 compared to normal air-exposed WT
42
43 482 controls.
44
45
46
47
48
49
50
51

52 484

53 485 **Figure 4: IL-22⁺ CD4⁺ T-cells, $\gamma\delta$ T-cells, NKT-cells and ILC3s are increased in**
54 **the lungs of CS-exposed mice with experimental COPD.** *Il17a^{eGFP/+};Il22^{td-tomato/+}*
55
56 486 reporter mice were exposed to normal air or CS for 8 weeks and the cellular source
57
58 487 of IL-17A and IL-22 in the lung was assessed by flow cytometry. (a) Representative
59
60 488

1
2
3 489 FACS plot of IL-17A⁺ and IL-22⁺ CD4⁺ T-cells. Total numbers of (b) IL-17A⁺, (c) IL-
4
5 490 22⁺ and (d) IL-17A⁺IL-22⁺ CD4⁺ T-cells in the lung. (e) Representative FACS plot of
6
7 491 IL-17A⁺ and IL-22⁺ $\gamma\delta$ T-cells. Total numbers of (f) IL-17A⁺, (g) IL-22⁺ and (h) IL-
8
9 492 17A⁺IL-22⁺ $\gamma\delta$ T-cells in the lung. (i) Representative FACS plot of IL-17A⁺ and IL-22⁺
10
11 493 NKT-cells. Total numbers of (j) IL-17A⁺, (k) IL-22⁺ and (l) IL-17A⁺IL-22⁺ NKT-cells in
12
13 494 the lung. (m) Representative FACS plot of IL-17A⁺ and IL-22⁺ ILC3s. Total numbers
14
15 495 of (n) IL-17A⁺, (o) IL-22⁺ and (p) IL-17A⁺IL-22⁺ ILC3 cells in the lung. Relative
16
17 496 proportion of CD4⁺ T-cells, $\gamma\delta$ T-cells, NKT-cells and ILC3s expressing (q) IL-17A, (r)
18
19 497 IL-22 and (s) IL-17 and IL-22. Data are presented as mean \pm SEM, n = 6, with
20
21 498 another independent experiment showing similar results. Two-tailed Mann-Whitney t-
22
23 499 test was used to analyse differences between two groups, whereby * = p<0.05
24
25 500 compared to normal air-exposed controls.
26
27
28
29
30
31
32

31 501
32
33 502 **Figure 5: CS-induced pulmonary inflammation is reduced in *IL22*^{-/-} mice.** Wild-
34
35 503 type (WT) and IL-22-deficient (*IL22*^{-/-}) C57BL/6 mice were exposed to normal air or
36
37 504 CS for 8 weeks to induce experimental COPD. (a) Total leukocytes, (b)
38
39 505 macrophages, (c) neutrophils and (d) lymphocytes in bronchoalveolar lavage fluid
40
41 506 (BALF). (e) Representative images of parenchymal inflammatory cells. (f) Numbers
42
43 507 of parenchymal inflammatory cells per high powered field. (g) Representative images
44
45 508 of lung histopathology scoring. (h) Total histopathology score in lung sections and
46
47 509 scores specifically in the (i) airway, (j) vascular and (k) parenchymal regions. (l)
48
49 510 *Cxcl1*, (m) *Cxcl2* and (n) *Il17a* mRNA expression in lung homogenates. Data are
50
51 511 presented as mean \pm SEM, n = 6, with another independent experiment showing
52
53 512 similar results.. The one-way analysis of variance with Bonferroni post-test analysed
54
55
56
57
58
59
60

1
2
3 513 differences between 3 or more groups, whereby * = $p < 0.05$ compared to normal air-
4
5 514 exposed controls.
6
7

8 515
9
10 516 **Figure 6: CS-induced increases in airway epithelial area, collagen deposition**
11 **and emphysema-like alveolar enlargement do not occur in *IL22*^{-/-} mice.** Wild-type
12 517 (WT) and IL-22-deficient (*IL22*^{-/-}) C57BL/6 mice were exposed to normal air or CS for
13 518 8 weeks to induce experimental COPD. (a) Representative images of small airway
14 519 epithelium. (b) Small airway epithelial thickness in terms of epithelial cell area (μm^2)
15 520 per basement membrane (BM) perimeter (μm). (c) Representative images of
16 521 collagen deposition around small airways. (d) Area of collagen deposition (μm^2) per
17 522 BM perimeter (μm). (e) Representative images of alveolar structure. (f) Alveolar
18 523 diameter (μm). Data are presented as mean \pm SEM, $n = 6$, with another independent
19 524 experiment showing similar results. The one-way analysis of variance with
20 525 Bonferroni post-test analysed differences between 3 or more groups, whereby * =
21 526 $p < 0.05$ compared to normal air-exposed controls.
22 527
23
24
25
26
27
28
29
30
31
32
33
34
35
36
37
38
39

40 529 **Figure 7: CS-induced lung function impairment is improved in *IL22*^{-/-} mice.** Wild-
41 530 type (WT) and IL-22-deficient (*IL22*^{-/-}) C57BL/6 mice were exposed to normal air or
42 531 CS for 8 weeks to induce experimental COPD. Lung function was assessed in terms
43 532 of (a) lung volume from pressure volume loops, (b) airway resistance, (c) total lung
44 533 capacity, (d) inspiratory capacity, (e) forced vital capacity and (f) compliance. Data
45 534 are presented as mean \pm SEM, $n = 6$, with another independent experiment showing
46 535 similar results. The one-way analysis of variance with Bonferroni post-test analysed
47 536 differences between 3 or more groups, whereby * = $p < 0.05$ compared to normal air-
48 537 exposed controls.
49
50
51
52
53
54
55
56
57
58
59
60

538 **References**

1. Lozano R, Naghavi M, Foreman K, Lim S, Shibuya K, Aboyans V, Abraham J, Adair T, Aggarwal R, Ahn SY, Alvarado M, Anderson HR, Anderson LM, Andrews KG, Atkinson C, Baddour LM, Barker-Collo S, Bartels DH, Bell ML, Benjamin EJ, Bennett D, Bhalla K, Bikbov B, Bin Abdulhak A, Birbeck G, Blyth F, Bolliger I, Boufous S, Bucello C, Burch M, Burney P, Carapetis J, Chen H, Chou D, Chugh SS, Coffeng LE, Colan SD, Colquhoun S, Colson KE, Condon J, Connor MD, Cooper LT, Corriere M, Cortinovis M, de Vaccaro KC, Couser W, Cowie BC, Criqui MH, Cross M, Dabhadkar KC, Dahodwala N, De Leo D, Degenhardt L, Delossantos A, Denenberg J, Des Jarlais DC, Dharmaratne SD, Dorsey ER, Driscoll T, Duber H, Ebel B, Erwin PJ, Espindola P, Ezzati M, Feigin V, Flaxman AD, Forouzanfar MH, Fowkes FG, Franklin R, Fransen M, Freeman MK, Gabriel SE, Gakidou E, Gaspari F, Gillum RF, Gonzalez-Medina D, Halasa YA, Haring D, Harrison JE, Havmoeller R, Hay RJ, Hoen B, Hotez PJ, Hoy D, Jacobsen KH, James SL, Jasrasaria R, Jayaraman S, Johns N, Karthikeyan G, Kassebaum N, Keren A, Khoo JP, Knowlton LM, Kobusingye O, Koranteng A, Krishnamurthi R, Lipnick M, Lipshultz SE, Ohno SL, Mabweijano J, MacIntyre MF, Mallinger L, March L, Marks GB, Marks R, Matsumori A, Matzopoulos R, Mayosi BM, McAnulty JH, McDermott MM, McGrath J, Mensah GA, Merriman TR, Michaud C, Miller M, Miller TR, Mock C, Mocumbi AO, Mokdad AA, Moran A, Mulholland K, Nair MN, Naldi L, Narayan KM, Nasseri K, Norman P, O'Donnell M, Omer SB, Ortblad K, Osborne R, Ozgediz D, Pahari B, Pandian JD, Rivero AP, Padilla RP, Perez-Ruiz F, Perico N, Phillips D, Pierce K, Pope CA, 3rd, Porrini E, Pourmalek F, Raju M, Ranganathan D, Rehm JT, Rein DB, Remuzzi G, Rivara FP, Roberts T, De Leon FR, Rosenfeld LC, Rushton L, Sacco RL, Salomon JA, Sampson U, Sanman E, Schwebel DC, Segui-Gomez M, Shepard DS, Singh D, Singleton J, Sliwa K, Smith E, Steer A, Taylor JA, Thomas B, Tleyjeh IM, Towbin JA, Truelsen T, Undurraga EA, Venketasubramanian N, Vijayakumar L, Vos T, Wagner GR, Wang M, Wang W, Watt K, Weinstock MA, Weintraub R, Wilkinson JD, Woolf AD, Wulf S, Yeh PH, Yip P, Zabetian A, Zheng ZJ, Lopez AD, Murray CJ, AlMazroa MA, Memish ZA. Global and regional mortality from 235 causes of death for 20 age groups in 1990 and 2010: a systematic analysis for the Global Burden of Disease Study 2010. *Lancet (London, England)* 2012; 380(9859): 2095-2128.
2. Keely S, Talley NJ, Hansbro PM. Pulmonary-intestinal cross-talk in mucosal inflammatory disease. *Mucosal immunology* 2012; 5(1): 7-18.
3. Barnes PJ. Corticosteroid resistance in patients with asthma and chronic obstructive pulmonary disease. *The Journal of allergy and clinical immunology* 2013; 131(3): 636-645.
4. Fricker M GB, Mateer S, Jones B, Kim RY, Gellatly SL, Jarnicki AG, Powell N, Oliver BG, Radford-Smith G, Talley NJ, Walker MM, Keely S, Hansbro PM. . Chronic smoke exposure induces systemic hypoxia that drives intestinal dysfunction. . *JCI insight* 2018(In Press).
5. Budden KF, Gellatly SL, Wood DL, Cooper MA, Morrison M, Hugenholtz P, Hansbro PM. Emerging pathogenic links between microbiota and the gut-lung axis. *Nature reviews Microbiology* 2017; 15(1): 55-63.
6. Dudakov JA, Hanash AM, van den Brink MR. Interleukin-22: immunobiology and pathology. *Annual review of immunology* 2015; 33: 747-785.

- 1
2
3
4 585 7. Xu W, Presnell SR, Parrish-Novak J, Kindsvogel W, Jaspers S, Chen Z, Dillon
586 SR, Gao Z, Gilbert T, Madden K, Schlutsmeyer S, Yao L, Whitmore TE,
587 Chandrasekher Y, Grant FJ, Maurer M, Jelinek L, Storey H, Brender T, Hammond A,
588 Topouzis S, Clegg CH, Foster DC. A soluble class II cytokine receptor, IL-22RA2, is
589 a naturally occurring IL-22 antagonist. *Proceedings of the National Academy of*
590 *Sciences of the United States of America* 2001; 98(17): 9511-9516.
- 591 8. Le Rouzic O, Pichavant M, Frealle E, Guillon A, Si-Tahar M, Gosset P. Th17
592 cytokines: novel potential therapeutic targets for COPD pathogenesis and
593 exacerbations. *The European respiratory journal* 2017; 50(4).
- 594 9. Guillon A, Jouan Y, Brea D, Gueugnon F, Dalloneau E, Baranek T, Henry C,
595 Morello E, Renauld JC, Pichavant M, Gosset P, Courty Y, Diot P, Si-Tahar M.
596 Neutrophil proteases alter the interleukin-22-receptor-dependent lung antimicrobial
597 defence. *The European respiratory journal* 2015; 46(3): 771-782.
- 598 10. Sharan R, Perez-Cruz M, Kervoaze G, Gosset P, Weynants V, Godfroid F,
599 Hermand P, Trottein F, Pichavant M, Gosset P. Interleukin-22 protects against non-
600 typeable *Haemophilus influenzae* infection: alteration during chronic obstructive
601 pulmonary disease. *Mucosal immunology* 2017; 10(1): 139-149.
- 602 11. Pichavant M, Sharan R, Le Rouzic O, Olivier C, Hennegrave F, Remy G,
603 Perez-Cruz M, Kone B, Gosset P, Just N, Gosset P. IL-22 Defect During
604 *Streptococcus pneumoniae* Infection Triggers Exacerbation of Chronic Obstructive
605 Pulmonary Disease. *EBioMedicine* 2015; 2(11): 1686-1696.
- 606 12. Beckett EL, Stevens RL, Jarnicki AG, Kim RY, Hanish I, Hansbro NG, Deane
607 A, Keely S, Horvat JC, Yang M, Oliver BG, van Rooijen N, Inman MD, Adachi R,
608 Soberman RJ, Hamadi S, Wark PA, Foster PS, Hansbro PM. A new short-term
609 mouse model of chronic obstructive pulmonary disease identifies a role for mast cell
610 tryptase in pathogenesis. *The Journal of allergy and clinical immunology* 2013;
611 131(3): 752-762.
- 612 13. Haw TJ, Starkey MR, Pavlidis S, Fricker M, Arthurs AL, Mono Nair P, Liu G,
613 Hanish I, Kim RY, Foster PS, Horvat JC, Adcock IM, Hansbro PM. Toll-like receptor
614 2 and 4 have Opposing Roles in the Pathogenesis of Cigarette Smoke-induced
615 Chronic Obstructive Pulmonary Disease. *American journal of physiology Lung*
616 *cellular and molecular physiology* 2017; ajplung.00154.02017.
- 617 14. Haw TJ, Starkey MR, Nair PM, Pavlidis S, Liu G, Nguyen DH, Hsu AC,
618 Hanish I, Kim RY, Collison AM, Inman MD, Wark PA, Foster PS, Knight DA, Mattes
619 J, Yagita H, Adcock IM, Horvat JC, Hansbro PM. A pathogenic role for tumor
620 necrosis factor-related apoptosis-inducing ligand in chronic obstructive pulmonary
621 disease. *Mucosal immunology* 2016; 9(4): 859-872.
- 622 15. Hsu AC, Starkey MR, Hanish I, Parsons K, Haw TJ, Howland LJ, Barr I,
623 Mahony JB, Foster PS, Knight DA, Wark PA, Hansbro PM. Targeting PI3K-
624 p110alpha Suppresses Influenza Virus Infection in Chronic Obstructive Pulmonary
625 Disease. *American journal of respiratory and critical care medicine* 2015; 191(9):
626 1012-1023.
- 627 16. Hsu AC, Dua K, Starkey MR, Haw TJ, Nair PM, Nichol K, Zammit N, Grey ST,
628 Baines KJ, Foster PS, Hansbro PM, Wark PA. MicroRNA-125a and -b inhibit A20
629 and MAVS to promote inflammation and impair antiviral response in COPD. *JCI*
630 *insight* 2017; 2(7): e90443.
- 631 17. Liu G, Cooley MA, Jarnicki AG, Hsu AC, Nair PM, Haw TJ, Fricker M, Gellatly
632 SL, Kim RY, Inman MD, Tjin G, Wark PA, Walker MM, Horvat JC, Oliver BG,
633 Argraves WS, Knight DA, Burgess JK, Hansbro PM. Fibulin-1 regulates the
634 pathogenesis of tissue remodeling in respiratory diseases. *JCI insight* 2016; 1(9).

- 1
2
3
4
5
6
7
8
9
10
11
12
13
14
15
16
17
18
19
20
21
22
23
24
25
26
27
28
29
30
31
32
33
34
35
36
37
38
39
40
41
42
43
44
45
46
47
48
49
50
51
52
53
54
55
56
57
58
59
60
- 635 18. Hansbro PM, Hamilton MJ, Fricker M, Gellatly SL, Jarnicki AG, Zheng D, Frei
636 SM, Wong GW, Hamadi S, Zhou S, Foster PS, Krillis SA, Stevens RL. Importance of
637 mast cell Prss31/transmembrane tryptase/tryptase-gamma in lung function and
638 experimental chronic obstructive pulmonary disease and colitis. *The Journal of*
639 *biological chemistry* 2014; 289(26): 18214-18227.
- 640 19. Plank MW, Kaiko GE, Maltby S, Weaver J, Tay HL, Shen W, Wilson MS,
641 Durum SK, Foster PS. Th22 Cells Form a Distinct Th Lineage from Th17 Cells In
642 Vitro with Unique Transcriptional Properties and Tbet-Dependent Th1 Plasticity.
643 *Journal of immunology (Baltimore, Md : 1950)* 2017; 198(5): 2182-2190.
- 644 20. Carolan BJ, Heguy A, Harvey BG, Leopold PL, Ferris B, Crystal RG. Up-
645 regulation of expression of the ubiquitin carboxyl-terminal hydrolase L1 gene in
646 human airway epithelium of cigarette smokers. *Cancer research* 2006; 66(22):
647 10729-10740.
- 648 21. Harvey BG, Heguy A, Leopold PL, Carolan BJ, Ferris B, Crystal RG.
649 Modification of gene expression of the small airway epithelium in response to
650 cigarette smoking. *Journal of molecular medicine (Berlin, Germany)* 2007; 85(1): 39-
651 53.
- 652 22. Campbell JD, McDonough JE, Zeskind JE, Hackett TL, Pechkovsky DV,
653 Brandsma CA, Suzuki M, Gosselink JV, Liu G, Alekseyev YO, Xiao J, Zhang X,
654 Hayashi S, Cooper JD, Timens W, Postma DS, Knight DA, Lenburg ME, Hogg JC,
655 Spira A. A gene expression signature of emphysema-related lung destruction and its
656 reversal by the tripeptide GHK. *Genome medicine* 2012; 4(8): 67.
- 657 23. Fricker M, Deane A, Hansbro PM. Animal models of chronic obstructive
658 pulmonary disease. *Expert opinion on drug discovery* 2014; 9(6): 629-645.
- 659 24. Jones B, Donovan C, Liu G, Gomez HM, Chimankar V, Harrison CL,
660 Wiegman CH, Adcock IM, Knight DA, Hirota JA, Hansbro PM. Animal models of
661 COPD: What do they tell us? *Respirology (Carlton, Vic)* 2017; 22(1): 21-32.
- 662 25. Starkey MR, Essilfie AT, Horvat JC, Kim RY, Nguyen DH, Beagley KW,
663 Mattes J, Foster PS, Hansbro PM. Constitutive production of IL-13 promotes early-
664 life Chlamydia respiratory infection and allergic airway disease. *Mucosal immunology*
665 2013; 6(3): 569-579.
- 666 26. Starkey MR, Nguyen DH, Essilfie AT, Kim RY, Hatchwell LM, Collison AM,
667 Yagita H, Foster PS, Horvat JC, Mattes J, Hansbro PM. Tumor necrosis factor-
668 related apoptosis-inducing ligand translates neonatal respiratory infection into
669 chronic lung disease. *Mucosal immunology* 2014; 7(3): 478-488.
- 670 27. Kedzierski L, Tate MD, Hsu AC, Kolesnik TB, Linossi EM, Dagley L, Dong Z,
671 Freeman S, Infusini G, Starkey MR, Bird NL, Chatfield SM, Babon JJ, Huntington N,
672 Belz G, Webb A, Wark PA, Nicola NA, Xu J, Kedzierska K, Hansbro PM, Nicholson
673 SE. Suppressor of cytokine signaling (SOCS)5 ameliorates influenza infection via
674 inhibition of EGFR signaling. *eLife* 2017; 6.
- 675 28. Essilfie AT, Horvat JC, Kim RY, Mayall JR, Pinkerton JW, Beckett EL, Starkey
676 MR, Simpson JL, Foster PS, Gibson PG, Hansbro PM. Macrolide therapy
677 suppresses key features of experimental steroid-sensitive and steroid-insensitive
678 asthma. *Thorax* 2015; 70(5): 458-467.
- 679 29. Nair PM, Starkey MR, Haw TJ, Liu G, Horvat JC, Morris JC, Verrills NM, Clark
680 AR, Ammit AJ, Hansbro PM. Targeting PP2A and proteasome activity ameliorates
681 features of allergic airway disease in mice. *Allergy* 2017; 72(12): 1891-1903.
- 682 30. Horvat JC, Beagley KW, Wade MA, Preston JA, Hansbro NG, Hickey DK,
683 Kaiko GE, Gibson PG, Foster PS, Hansbro PM. Neonatal chlamydial infection

- 1
2
3 684 induces mixed T-cell responses that drive allergic airway disease. *American journal*
4 685 *of respiratory and critical care medicine* 2007: 176(6): 556-564.
- 5
6 686 31. Tam A, Hughes M, McNagny KM, Obeidat M, Hackett TL, Leung JM,
7 687 Shaipanich T, Dorscheid DR, Singhera GK, Yang CWT, Pare PD, Hogg JC, Nickle
8 688 D, Sin DD. Hedgehog signaling in the airway epithelium of patients with chronic
9 689 obstructive pulmonary disease. *Scientific reports* 2019: 9(1): 3353.
- 10 690 32. Horvat JC, Starkey MR, Kim RY, Phipps S, Gibson PG, Beagley KW, Foster
11 691 PS, Hansbro PM. Early-life chlamydial lung infection enhances allergic airways
12 692 disease through age-dependent differences in immunopathology. *The Journal of*
13 693 *allergy and clinical immunology* 2010: 125(3): 617-625, 625.e611-625.e616.
- 14 694 33. Kim RY, Horvat JC, Pinkerton JW, Starkey MR, Essilfie AT, Mayall JR, Nair
15 695 PM, Hansbro NG, Jones B, Haw TJ, Sunkara KP, Nguyen TH, Jarnicki AG, Keely S,
16 696 Mattes J, Adcock IM, Foster PS, Hansbro PM. MicroRNA-21 drives severe, steroid-
17 697 insensitive experimental asthma by amplifying phosphoinositide 3-kinase-mediated
18 698 suppression of histone deacetylase 2. *The Journal of allergy and clinical immunology*
19 699 2017: 139(2): 519-532.
- 20 700 34. Kim RY, Pinkerton JW, Essilfie AT, Robertson AAB, Baines KJ, Brown AC,
21 701 Mayall JR, Ali MK, Starkey MR, Hansbro NG, Hirota JA, Wood LG, Simpson JL,
22 702 Knight DA, Wark PA, Gibson PG, O'Neill LAJ, Cooper MA, Horvat JC, Hansbro PM.
23 703 Role for NLRP3 Inflammasome-mediated, IL-1beta-Dependent Responses in
24 704 Severe, Steroid-Resistant Asthma. *American journal of respiratory and critical care*
25 705 *medicine* 2017: 196(3): 283-297.
- 26 706 35. Vogelmeier CF, Criner GJ, Martinez FJ, Anzueto A, Barnes PJ, Bourbeau J,
27 707 Celli BR, Chen R, Decramer M, Fabbri LM, Frith P, Halpin DM, Lopez Varela MV,
28 708 Nishimura M, Roche N, Rodriguez-Roisin R, Sin DD, Singh D, Stockley R, Vestbo J,
29 709 Wedzicha JA, Agusti A. Global Strategy for the Diagnosis, Management, and
30 710 Prevention of Chronic Obstructive Lung Disease 2017 Report. GOLD Executive
31 711 Summary. *American journal of respiratory and critical care medicine* 2017: 195(5):
32 712 557-582.
- 33 713 36. Shan M, Yuan X, Song LZ, Roberts L, Zarinkamar N, Seryshev A, Zhang Y,
34 714 Hilsenbeck S, Chang SH, Dong C, Corry DB, Kheradmand F. Cigarette smoke
35 715 induction of osteopontin (SPP1) mediates T(H)17 inflammation in human and
36 716 experimental emphysema. *Science translational medicine* 2012: 4(117): 117ra119.
- 37 717 37. Aujla SJ, Dubin PJ, Kolls JK. Interleukin-17 in pulmonary host defense.
38 718 *Experimental lung research* 2007: 33(10): 507-518.
- 39 719 38. Shukla SD, Budden KF, Neal R, Hansbro PM. Microbiome effects on
40 720 immunity, health and disease in the lung. *Clinical & translational immunology* 2017:
41 721 6(3): e133.
- 42 722 39. Budden KF, Shukla SD, Rehman SF, Bowerman KL, Keely S, Hugenholtz P,
43 723 Armstrong-James DPH, Adcock IM, Chotirmall SH, Chung KF, PM. H. Functional
44 724 effects of microbiota in chronic respiratory disease. . *Lancet Respiratory Medicine*
45 725 2019: In press.
- 46 726 40. Pichavant M, Remy G, Bekaert S, Le Rouzic O, Kervoaze G, Vilain E, Just N,
47 727 Tillie-Leblond I, Trottein F, Cataldo D, Gosset P. Oxidative stress-mediated iNKT-cell
48 728 activation is involved in COPD pathogenesis. *Mucosal immunology* 2014: 7(3): 568-
49 729 578.
- 50 730 41. De Grove KC, Provoost S, Verhamme FM, Bracke KR, Joos GF, Maes T,
51 731 Brusselle GG. Characterization and Quantification of Innate Lymphoid Cell Subsets
52 732 in Human Lung. *PloS one* 2016: 11(1): e0145961.

- 1
2
3
4 733 42. Thatcher TH, McHugh NA, Egan RW, Chapman RW, Hey JA, Turner CK,
5 734 Redonnet MR, Seweryniak KE, Sime PJ, Phipps RP. Role of CXCR2 in cigarette
6 735 smoke-induced lung inflammation. *American journal of physiology Lung cellular and*
7 736 *molecular physiology* 2005; 289(2): L322-328.
- 8 737 43. Meijer M, Rijkers GT, van Overveld FJ. Neutrophils and emerging targets for
9 738 treatment in chronic obstructive pulmonary disease. *Expert review of clinical*
10 739 *immunology* 2013; 9(11): 1055-1068.
- 11 740 44. Li JR, Zhou WX, Huang KW, Jin Y, Gao JM. Interleukin-22 exacerbates
12 741 airway inflammation induced by short-term exposure to cigarette smoke in mice.
13 742 *Acta pharmacologica Sinica* 2014; 35(11): 1393-1401.
- 14 743 45. Pociask DA, Scheller EV, Mandalapu S, McHugh KJ, Enelow RI, Fattman CL,
15 744 Kolls JK, Alcorn JF. IL-22 is essential for lung epithelial repair following influenza
16 745 infection. *The American journal of pathology* 2013; 182(4): 1286-1296.
- 17 746 46. Wang S, Li Y, Fan J, Zhang X, Luan J, Bian Q, Ding T, Wang Y, Wang Z,
18 747 Song P, Cui D, Mei X, Ju D. Interleukin-22 ameliorated renal injury and fibrosis in
19 748 diabetic nephropathy through inhibition of NLRP3 inflammasome activation. *Cell*
20 749 *death & disease* 2017; 8(7): e2937.

21
22
23 750
24
25
26
27
28
29
30
31
32
33
34
35
36
37
38
39
40
41
42
43
44
45
46
47
48
49
50
51
52
53
54
55
56
57
58
59
60

1 IL-22 and its receptors are increased in human and 2 experimental COPD and contribute to pathogenesis

3 Malcolm R. Starkey¹, Maximilian W. Plank¹, Paolo Casolari², Alberto Papi², Stelios
4 Pavlidis³, Yike Guo³, Guy J.M. Cameron¹, Tatt Jhong Haw¹, [Anthony Tam^{4,5}](#), [Ma'en
5 Obiedat^{4,5}](#), Chantal Donovan¹, Nicole G. Hansbro^{1,64} Duc H. Nguyen¹, Prema Mono
6 Nair¹, Richard Y. Kim¹, Jay C. Horvat¹, Gerard E. Kaiko¹, Scott K. Durum⁵, Peter A.
7 Wark¹, [Don D. Sin^{4,5}](#), Gaetano Caramori⁸⁶, Ian M. Adcock³, Paul S. Foster¹ and
8 Philip M. Hansbro^{1,64}

9
10 **Affiliations:** ¹Priority Research Centre for Healthy Lungs, School of Biomedical
11 Sciences and Pharmacy, Hunter Medical Research Institute & University of
12 Newcastle, Callaghan, New South Wales, Australia. ²Interdepartmental Study Center
13 for Inflammatory and Smoke-related Airway Diseases (CEMICEF), Cardiorespiratory
14 and Internal Medicine Section, University of Ferrara, Ferrara, Italy. ³The Airways
15 Disease Section, National Heart & Lung Institute, Imperial College London, London,
16 UK. [4The University of British Columbia Center for Heart Lung Innovation, St Paul's
17 Hospital, Vancouver, Canada.](#) [5Respiratory Division, Department of Medicine,
18 University of British Columbia, Vancouver, BC.](#) [6Centre for inflammation, Centenary
19 Institute, Sydney, and School of Life Sciences, University of Technology, Ultimo,
20 NSW, Australia.](#) ⁶⁴Centre for inflammation, Centenary Institute, Sydney, and School
21 of Life Sciences, University of Technology, Ultimo, NSW, Australia. ⁷⁵Laboratory of
22 Immunoregulation, Cancer and Inflammation Program, Center for Cancer Research,
23 National Cancer Institute, National Institutes of Health, Frederick, MD, USA. ⁸⁶UOC

1
2
3 24 di Pneumologia, Dipartimento di Scienze Biomediche, Odontoiatriche e delle
4
5 25 Immagini Morfologiche e Funzionali (BIOMORF), Università di Messina, Italy.
6
7

8 26 **Correspondence:** Professor Philip M. Hansbro, Centre for inflammation, Centenary
9
10 27 Institute, Sydney, and School of Life Sciences, University of Technology, Ultimo,
11
12 28 NSW, Australia. E-mail: p.hansbro@centenary.org.au
13
14
15 29

17 30 **Supplementary methods**

21 31 **Ethics statement.** This study was performed in accordance with the
22
23 32 recommendations issued by the National Health and Medical Research Council of
24
25 33 Australia. All experimental protocols were approved by the animal ethics committee
26
27 34 of The University of Newcastle, Australia.
28
29
30
31 35

34 36 **Gene Expression in Human COPD Microarray Datasets.** Analysis of IL-22, IL-
35
36 37 22RA1 IL-10RB and IL-22RA2 in published human array datasets (Affymetrix Human
37
38 38 Genome U133 Plus 2.0 Array, Accession numbers: GSE5058 and GSE27597) [1-3]
39
40 39 was performed using the Array Studio software (Omicsoft Corporation, Research
41
42 40 Triangle Park, NC, USA) by applying a general linear model adjusting for age and
43
44 41 gender and the Benjamini–Hochberg method for p-value adjustment. Data are
45
46 42 expressed as \log_2 intensity robust multi-array average signals. The Benjamini–
47
48 43 Hochberg method for adjusted P value/false discovery rate (FDR) was used to
49
50 44 analyse differences between two groups. Statistical significance was set at FDR <
51
52 45 0.05.
53
54
55 46

57 46 In the GSE5058 dataset, gene arrays from small airway epithelial cells
58
59 47 obtained from normal non-smokers (n = 12), healthy chronic smokers (n = 12),
60

1
2
3 48 smokers with early COPD (n=9), and smokers with established COPD (n = 6) were
4
5 49 evaluated. The FEV1/FVC ratio of the subjects in these groups were 99 ± 7 , 97 ± 7 ,
6
7
8 50 78 ± 4 and 66 ± 14 , respectively.

9
10 51 In the GSE27597 dataset, gene arrays from 8 sample pairs from different lung
11
12 52 slices from 6 subjects requiring lung transplant for COPD and 2 organ donors were
13
14
15 53 analysed. The 6 subjects with COPD had a FEV1 <25% predicted (severe disease).

16
17 54 In addition, we examined gene expression from lung tissue specimens
18
19 55 derived from 56 subjects (GSE8581 [4]). These subjects had undergone lobectomy
20
21 56 for removal of a suspected tumour. Tissue was derived from histologically normal
22
23
24 57 tissue distant from the tumour margin. COPD (cases, n = 15) were defined as
25
26 58 subjects with FEV1<70% and FEV1/FVC<0.7 and controls (n = 18) as subjects with
27
28 59 FEV1>80% and FEV1/FVC>0.7.

30
31 60
32
33
34 61 **Mice.** Female, 7-8-week-old, wild-type (WT) C57BL/6, *Il17a^{eGFP/+};Il22^{td-tomato/+}*
35
36 62 reporter and *Il22^{-/-}* mice were obtained from the Australian Bioresource Facility, Moss
37
38 63 Vale, NSW, Australia. *Il17a^{eGFP/+}Il22^{td-tomato/+}* dual reporter and *Il22^{-/-}* and mice were
39
40 64 generated as previously described [5]. Mice were housed under a 12-hour light/dark
41
42 65 cycle and had free access to food (standard chow) and water. After a period of
43
44 66 acclimatization (5 days), mice were randomly placed into experimental groups and
45
46 67 exposed to either normal air or nose-only inhalation of CS for eight weeks as
47
48 68 described previously [6-13].

49
50
51 69
52
53
54
55
56 70 **Isolation of RNA and qPCR.** Total RNA was extracted from whole lung tissue and
57
58 71 blunt-dissected airways and parenchyma and reversed transcribed [8]. mRNA
59
60

1
2
3 72 transcripts were determined by real-time quantitative PCR (qPCR, ABIPrism7000,
4
5 73 Applied Biosystems, Scoresby, Victoria, Australia) using custom designed primers
6
7 74 (Integrated DNA Technologies, Baulkham Hills, New South Wales, Australia),
8
9 75 normalized to the reference gene hypoxanthine-guanine phosphoribosyltransferase
10
11 76 (*hprt*) (**supplementary table 1**).

12
13
14
15 77

16
17
18 78 **Flow Cytometry Analysis.** The numbers of IL-17A⁺ and IL-22⁺ CD4⁺ T-cells, $\gamma\delta$ T-
19
20 79 cells, NKT-cells and group 3 innate lymphoid cells in lung homogenates were
21
22 80 determined based on surface marker expression using flow cytometry
23
24 81 (**supplementary table 2**) [14-16]. Flow cytometric analysis was performed using a
25
26 82 FACSriaIII with FACSDiva software (BD Biosciences, North Ryde, Australia). Flow
27
28 83 cytometry antibodies were purchased from Biolegend (Karrinyup, Western Australia,
29
30 84 Australia) or BD Biosciences (**supplementary table 3**). BD compensation beads
31
32 85 (BD Biosciences) were used to compensate for spectral overlap.
33
34
35
36
37
38
39

40
41 86

42
43 87 **Mouse lung IHC.** Lungs were perfused, inflated, formalin fixed, paraffin embedded,
44
45 88 and sectioned (4 μ m)[8, 9]. Longitudinal sections of the left lung were deparaffinised
46
47 89 by placing on a heating block at 70°C for 15mins then sections were immersed in
48
49 90 fresh xylene for 10mins then 5mins. Rehydration was performed using a series of
50
51 91 ethanol gradients (100% twice, 90%, 80%, 70%) and 0.85% saline for 5mins each.
52
53 92 Heat-induced antigen retrieval was performed in citrate buffer (10mM citric acid,
54
55 93 0.05% Tween 20, pH 6.0) at 100°C for 30mins. Sections were blocked with casein
56
57 94 blocker (Thermo Fisher Scientific, Scoresby, Victoria, Australia) for 1h. Sections
58
59 95 were washed with PBS-T and incubated overnight at 4°C with either rat anti-IL22ra1
60

1
2
3 96 (MAB42941; R&D Systems, Minneapolis, Minnesota, United States) or rabbit anti-
4
5 97 Il22ra2 (ab203211; Abcam, Melbourne, Victoria, Australia) antibodies. Following
6
7 98 washing with PBS-T, sections were incubated for 30mins at 37°C with either goat
8
9 99 anti-rat (HAF005; R&D Systems) or goat-anti-rabbit (ab7090; Abcam) secondary
10
11 100 antibodies conjugated to horseradish peroxidase. Each primary and secondary
12
13 101 antibody was diluted 1:100 in PBS-T. Following washing with PBS-T, sections were
14
15 102 incubated for 20 mins with 3,3'-diaminobenzidine chromogen-substrate buffer
16
17 103 (Aligent Technologies, Mulgrave, Victoria, Australia) according to the manufacturer's
18
19 104 instructions. Sections were washed with ddH₂O then counterstained with standard
20
21 105 haematoxylin for 5mins. Sections were washed with tap H₂O and were dehydrated
22
23 106 by immersion in a series of saline, ethanol then xylene, inverse to that described
24
25 107 above. Coverslips were mounted with standard non-aqueous medium and slides
26
27 108 imaged using a Zeiss Axio microscope with ZEN-blue edition software V2.5 (Carl
28
29 109 Zeiss Microscopy, Thornwood, New York, United States). Unless otherwise stated,
30
31 110 each incubation was at room temperature protected from light in a humidified
32
33 111 chamber. All wash steps were performed 5 times for 3mins each.
34
35
36
37
38
39
40
41
42

43 113 **Airway remodelling.** Airway epithelial (μm^2) and collagen deposition area (μm^2)
44
45 114 were assessed in a minimum of four small airways (basement membrane [BM]
46
47 115 perimeter $<1,000\mu\text{m}$) per section [7-9, 12, 13]. Lung sections were stained using
48
49 116 Masson's trichrome stain, and photographs of small intact airways were taken at 40x
50
51 117 magnification. These photographs were then analysed in ImageJ software (Version
52
53 118 1.50, NIH).

54
55
56
57 119 Airway epithelial thickness analysis was performed by carefully tracing the BM
58
59 120 and inner epithelial surface perimeters. Airway epithelial area was calculated by

1
2
3 121 subtracting the inner airway area from the outer airway area. This was then
4
5 122 expressed as area per μm of BM.
6
7

8 123 For collagen analysis, a colour deconvolution method was used to isolate the
9
10 124 collagen, stained blue. This method breaks the original photograph into three
11
12 125 images, containing three separate colour ranges. In this manner, the blue-stained
13
14 126 areas of the images (representing collagen) could be isolated and quantified
15
16 127 separately. The BM was traced and measured as described above.
17
18 128 Collagen deposition immediately surrounding the airway was traced and measured,
19
20 129 but only in images that isolated the blue-stained pixels. We could then reach a
21
22 130 quantitative 'collagen per airway' measurement by expressing the area of blue-
23
24 131 stained pixels per μm of BM.
25
26
27
28
29
30
31

32 133 **Pulmonary Inflammation.** Airway inflammation was assessed by differential
33
34 134 enumeration of inflammatory cells in bronchoalveolar lavage fluid (BALF) [7, 8, 17-
35
36 135 19]. BALF supernatants were stored at -20°C for assessment of IL-22 protein levels.
37
38 136 Lung sections were stained with periodic acid-Schiff (PAS) and tissue inflammation
39
40 137 assessed by enumeration of inflammatory cells [7, 8, 17, 18]. Histopathological score
41
42 138 was determined in lung sections stained with hematoxylin and eosin (H&E) based on
43
44 139 established custom-designed criteria [19].
45
46
47
48
49
50
51

52 141 **ELISA.** Right lung lobes were homogenised on ice in 500 μL of PBS supplemented
53
54 142 with Complete mini protease inhibitor cocktail (Roche Diagnostic, Sydney, NSW,
55
56 143 Australia) and PhosphoSTOP tablets (Roche Diagnostic). Lung homogenates were
57
58 144 incubated on ice for 5 mins and subsequently centrifuged (8,000 $\times g$, 15 mins).
59
60

1
2
3 145 Supernatants were collected, stored at -20°C overnight and total protein levels were
4
5 146 determined using Pierce BCA assay kit (Thermo Fisher Scientific) prior to ELISA. IL-
6
7 147 17A, IL-22, MPO and neutrophil elastase protein levels were quantified with
8
9 148 commercially available ELISA kits (R&D Systems or Biolegend) [5]. IL-22 protein
10
11 149 levels were normalised to total protein in lung homogenates.
12
13
14

15
16 150

17
18 151 **Lung Function.** Mice were anaesthetised with ketamine (100mg/kg) and xylazine
19
20 152 (10mg/kg, Troy Laboratories, Smithfield, Australia) prior to tracheostomy. Tracheas
21
22 153 were then cannulated and attached to Buxco® Forced Manoeuvres systems
23
24 154 apparatus (DSI, St. Paul, Minnesota, USA) to assess total lung capacity [7, 8]. Mice
25
26 155 were then attached to a FlexiVent apparatus (FX1 System; SCIREQ, Montreal,
27
28 156 Canada) to assess lung volume, airway resistance, inspiratory capacity, forced vital
29
30 157 capacity and compliance (tidal volume of 8mL/kg at a respiratory rate of 450
31
32 158 breaths/mins) [7, 20, 21]. All assessments were performed at least three times and
33
34 159 the average was calculated for each mouse.
35
36
37
38

39 160

40
41 161 **Human lung tissue study population.** Peripheral lung samples were obtained from
42
43 162 subjects undergoing lung resection for peripheral lung carcinoma from the
44
45 163 Respiratory Unit of the University Hospital of Ferrara, Italy (supplementary table 4).
46
47 164 Smokers with mild-to-moderate stable COPD (n=12) were compared with age- and
48
49 165 smoke history-matched smokers with normal lung function (NLF) (n=12). Diagnosis
50
51 166 of COPD was defined according to international guidelines as the presence of post-
52
53 167 bronchodilator FEV1/FVC ratio <70% or the presence of cough and sputum
54
55 168 production for at least 3 months in each of two consecutive years [22]. All patients
56
57 169 were in stable condition at the time of the surgery and had not suffered acute
58
59
60

1
2
3 170 exacerbations or upper respiratory tract infections in the preceding two months.
4
5 171 None had received glucocorticoids or antibiotics within the month preceding surgery,
6
7 172 or inhaled bronchodilators within the previous 48 h. Patients had no history of
8
9 173 asthma or other allergic diseases. All former smokers had stopped smoking for
10
11 174 more than one year. Each patient was subjected to medical history, physical
12
13 175 examination, chest radiography, electrocardiogram, routine blood tests, and
14
15 176 pulmonary function tests during the week prior to surgery. Pulmonary function tests
16
17 177 (Biomedin Spirometer, Padova, Italy) were performed as previously described [23]
18
19 178 according to published guidelines.
20
21
22
23
24
25
26

27 180 **Lung sample preparation and IHC.** Collection, processing, immunohistochemical
28
29 181 analysis of lung tissue samples as well as data analysis were performed as
30
31 182 previously published [24, 25]. The primary antibodies (anti-human) used are
32
33 183 summarised in supplementary table 5. Negative antibody controls used were
34
35 184 nonspecific isotype matched Ig at their respective primary antibody concentrations.
36
37 185 Image analysis was performed [24] using an integrated microscope (Olympus,
38
39 186 Albertslund, Denmark), video camera (JVC Digital color, Tatstrup, Denmark),
40
41 187 automated microscope stage (Olympus) and PC running Image pro-Plus Software
42
43 188 (Media Cybernetics) to quantify the RBP staining areas. Immunostaining counting
44
45 189 and interpretation were performed blinded without prior knowledge of clinical-
46
47 190 pathologic parameters.
48
49
50
51
52

53 191
54
55
56 192 **Scoring system for IHC in peripheral lung.** Staining analysis was performed as
57
58 193 previously published [24, 25]. A bronchiole was taken to be an airway with no
59
60

1
2
3 194 cartilage and glands in its wall. According to a validated method [24] the number of
4
5 195 positively stained endoalveolar macrophages was expressed as a percentage of the
6
7
8 196 total cells with the morphological appearance of alveolar macrophages counted
9
10 197 inside of the alveoli. The number of bronchiolar epithelial cells with positive staining
11
12 198 was expressed as a percentage of the total number of epithelial cells counted in
13
14 199 each bronchiolar section and group data were expressed as mean and standard
15
16
17 200 error of the mean (SEM). Airway epithelial-specific IL-22RA1 protein intensity was
18
19 201 quantified using the Aperio imaging system and normalized to the length of the
20
21 202 basement membrane.
22
23
24
25 203

26
27 204 **Statistical analyses.** Unless otherwise stated, data are presented as means \pm
28
29 205 standard error of mean (SEM) and are representative of two independent
30
31 206 experiments with 6 mice per group. The two-tailed Mann-Whitney test was used to
32
33 207 compare two groups. The one-way analysis of variance with Bonferroni post-test was
34
35 208 used to compare 3 or more groups. Statistical significance was set at $P < 0.05$ and
36
37 209 determined using GraphPad Prism Software version 6 (San Diego, CA, USA).
38
39
40
41
42 210
43
44
45
46
47
48
49
50
51
52
53
54
55
56
57
58
59
60

211 **Supplementary table 1.** Custom-designed primers used in qPCR analysis

Primer	Primer sequence (5' → 3')
<i>Il22ra1</i> forward	GTTTTACTACGCCAAGGTCACG
<i>Il22ra1</i> reverse	CACTTTGGGGATACAGGTCACA
<i>Il10rb</i> forward	ATTCGGAGTGGGTCAATGT
<i>Il10rb</i> reverse	CTGAGAAACGCAGGTGTAAAG
<i>Il22ra2</i> forward	CTCTTCTGTGACCTGACCAATGA
<i>Il22ra2</i> reverse	TTATAGTCACGACCGGAGGATCT
<i>Cxcl1</i> forward	GCTGGGATTCACCTCAAGAA
<i>Cxcl1</i> reverse	CTTGGGGACACCTTTTAGCA
<i>Cxcl2</i> forward	TGCTGCTGGCCACCAACCAC
<i>Cxcl2</i> reverse	AGTGTGACGCCCCCAGGACC
<i>Il17a</i> forward	GTGTCTCTGATGCTGTTGCT
<i>Il17a</i> reverse	GTTGACCTTCACATTCTGGA
<i>Hprt</i> forward	AGGCCAGACTTTGTTGGATTTGAA
<i>Hprt</i> reverse	CAACTTGCGCTCATCTTAGGATTT

212

1
2
3 214 **Supplementary table 2.** Surface antigens used to characterise mouse IL-17A⁺ IL-22⁺ lung
4
5 215 cell subsets by flow cytometry
6
7

Cell subset	Cell surface antigens
CD4 ⁺ T cells	CD45 ⁺ CD3 ⁺ CD4 ⁺ CD8 ⁻
$\gamma\delta$ T cells	CD45 ⁺ CD3 ⁺ $\gamma\delta$ TCR ⁺
NKT cells	CD45 ⁺ CD3 ⁺ α GalCer tetramer ⁺
ILC3	CD45 ⁺ CD3 ⁻ Ly6C/G ⁻ CD11b ⁻ B220 ⁻ TER119 ⁻ IL-7R α ⁺ CD90.2 ⁺
IL-17A and IL-22	Reported by eGFP and td-tomato, respectively

26
27 216
28
29
30
31
32
33
34
35
36
37
38
39
40
41
42
43
44
45
46
47
48
49
50
51
52
53
54
55
56
57
58
59
60

218 **Supplementary table 3.** Antibodies used in flow cytometry analysis

Cell surface antigens		Clone	Fluorophore	Company
CD45		30-F11	PerCP-Cy5.5	Biologend
CD3		17A2	AF700	Biologend
CD4		RM4-5	APC-Cy7	Biologend
CD8		53-6.7	BV510	Biologend
$\gamma\delta$ TCR		GL3	BV421	Biologend
α GalCer Tetramer		N/A	BV605	N/A
Lineage cocktail (CD3, CD11b, TER119)		17A2, Ly6C/G, B220, M1/70, RA3-6B2, Ter-119	AF700	Biologend

219

220 **Supplementary Table 4.** Characteristics of subjects for the immunohistochemical study of interleukins on peripheral lung
221

Subjects	N.	Age	Sex	Smoking history	Pack-years	Chronic bronchitis	FEV ₁ % pred	FEV ₁ /FVC %
Control smokers	12	70.8 ±2.3	10M/2F	8 Ex smokers 4 Current smokers	41.9 ±11.4	0	104.3±4.0	76.7±1.3
COPD	12	72.4 ±1.5	12M	7 Ex smokers 5 Current smokers	40.6 ±3.3	4 with chronic bronchitis	76.9±6.2	61.6±2.7

222

223 **Supplementary table 5.** Primary antibodies and immunohistochemical conditions used for
 224 identification of interleukins in the peripheral lung

Antigen	Company	Catalogue	Host	Concentration	Secondary antibody
IL10Rb	MyBio Source	MBS2003603	Rabbit	1.8 µg/ml	Goat anti-rabbit IgG, Vector (BA 1000); 1:200
IL-22	R&D	AF782	Goat	4 µg/ml	Rabbit anti-goat IgG, Vector (BA 5000); 1:200
IL22RA1 / IL22R	EMD Millipore/L SBio	06-1077- I/LS-B1365	Rabbit	2.2 µg/ml	Goat anti-rabbit IgG, Vector (BA 1000); 1:200
IL22RA2	Atlas	HPA030582	Rabbit	1 µg/ml	Goat anti-rabbit IgG, Vector (BA 1000); 1:200

225

226

227 **Supplementary table 6.** Immunohistochemical percentage of peripheral lung IL-22-positive
 228 cells

Localization and antigen	Control smokers	COPD	Mann-Whitney test p value
Bronchiolar epithelium			
Nuclear	8.3±2.8 5.0 (9.6) 1.0-13.8	9.0±2.5 5.0 (8.7) 2.0-18.0	0.6427
Cytosolic	48.5±7.0 54.5 (24.1) 25.3-70.3	60.8±6.6 67.5 (22.8) 44.5-76.3	0.2037
Alveolar macrophages			
Nuclear	16.7±4.1 11.5 (14.1)	46.5±7.5 51.0 (26.1)	0.0130
Cytosolic	9.0-23.0 62.0 (20.3)	28.3-63.5 58.0 (13.8)	0.0602

40.8-76.5 27.0-48.5

229 Data expressed as mean \pm SEM (first line), median (SD) (second line) and interquartile
 230 range (third line). Data expressed as mean \pm SEM (first line), median (SD) (second line) and
 231 interquartile range (third line).

232

233 **Supplementary table 7. Immunohistochemical percentage of peripheral lung IL22RA1-**
 234 **positive cells**

235

Localization and antigen	Control smokers	COPD	Mann-Whitney test p value
Bronchiolar epithelium			
Nuclear	3.8 \pm 2.3	24.9 \pm 4.6	0.0009
	0.8 (7.9)	24.5 (15.9)	
	0.0-4.0	16.8-27.5	
Cytosolic	30.5 \pm 7.8	8.2 \pm 3.5	0.0123
	21.5 (27.1)	2.0 (12.1)	
	7.0-57.3	0.0-16.8	
Alveolar macrophages			
Nuclear	1.9 \pm 0.9	20.7 \pm 4.3	0.0005
	0.5 (3.2)	21.0 (15.0)	
	0.0-2.8	5.5-35.3	
Cytosolic	0.0-2.8	5.5-35.3	0.0022
	72.5 \pm 3.9	52.0 \pm 3.9	
	75.0 (13.4)	49.0 (13.5)	

236 Data expressed as mean \pm SEM (first line), median (SD) (second line) and interquartile
 237 range (third line). Data expressed as mean \pm SEM (first line), median (SD) (second line) and
 238 interquartile range (third line).

239

240 **Supplementary table 8. Immunohistochemical percentage of peripheral lung IL22RA2-**
 241 **positive cells**

Localization and antigen	Control smokers	COPD	Mann-Whitney test p value
Bronchiolar epithelium			

Nuclear	0	0	-----
	0	0	
	0	0	
Cytosolic	25.7±7.0	11.8±3.7	0.1645
	19.0 (24.1)	8.0 (12.8)	
	3.5-49.5	1.3-20.5	
Alveolar macrophages			
Nuclear	0	0	-----
	0	0	
	0	0	
Cytosolic	47.5±5.0	48.2±8.5	0.8173
	46.5 (17.5)	52.5 (29.3)	
	34.3-59.8	22.5-73.3	

242 Data expressed as mean ± SEM (first line), median (SD) (second line) and interquartile
 243 range (third line). Data expressed as mean ± SEM (first line), median (SD) (second line) and
 244 interquartile range (third line).

245

246 **Supplementary table 9.** Immunohistochemical percentage of peripheral lung IL10Rb-
 247 positive cells

Localization and antigen	Control smokers	COPD	Mann-Whitney test p value
Bronchiolar epithelium			
Nuclear	1.8±0.8	3.4±1.1	0.1259
	0.5 (2.6)	2.0 (3.8)	
	0.0-2.8	1.0-4.8	
Cytosolic	27.0±7.6	26.9±5.3	0.7505
	16.0 (26.5)	18.5 (18.4)	
	2.8-58.3	13.0-41.8	
Alveolar macrophages			
Nuclear	5.5±1.7	19.1±3.7	0.0044
	5.0 (5.9)	19.0 (12.8)	

	0.0-11.8	7.5-25.0	
Cytosolic	59.8±5.9	59.6±4.0	0.9769
	62.0 (20.3)	58.0 (13.8)	
	38.5-76.5	49.3-66.8	

248 Data expressed as mean ± SEM (first line), median (SD) (second line) and interquartile
249 range (third line).

250

251 **Supplementary Table 10.** Characteristics of subjects for the IL-22RA1 intensity in airway
252 epithelial cells

Subjects	Non-smokers	Healthy smokers	GOLD 2	GOLD 3, 4
<u>Sex (M/F)</u>	<u>2/4</u>	<u>2/4</u>	<u>6/3</u>	<u>4/5</u>
<u>Smoking status (current/ex/NA)</u>	<u>0/0/0</u>	<u>4/2/0</u>	<u>4/3/2</u>	<u>1/8/0</u>
<u>Age (mean ± SD)</u>	<u>58.0±18.1</u>	<u>65.8±9.2</u>	<u>63.7±9.0</u>	<u>60.3±6.0</u>
<u>FEV1/FVC % (mean ± SD)</u>	<u>82.9±4.4</u>	<u>76.5±3.5</u>	<u>57.1±5.6</u>	<u>33.5±11.1</u>

253

254

255

256 References

- 257 1. Carolan BJ, Heguy A, Harvey BG, Leopold PL, Ferris B, Crystal RG. Up-
258 regulation of expression of the ubiquitin carboxyl-terminal hydrolase L1 gene in
259 human airway epithelium of cigarette smokers. *Cancer research* 2006; 66(22):
260 10729-10740.
- 261 2. Harvey BG, Heguy A, Leopold PL, Carolan BJ, Ferris B, Crystal RG.
262 Modification of gene expression of the small airway epithelium in response to
263 cigarette smoking. *Journal of molecular medicine (Berlin, Germany)* 2007; 85(1): 39-
264 53.
- 265 3. Campbell JD, McDonough JE, Zeskind JE, Hackett TL, Pechkovsky DV,
266 Brandsma CA, Suzuki M, Gosselink JV, Liu G, Alekseyev YO, Xiao J, Zhang X,
267 Hayashi S, Cooper JD, Timens W, Postma DS, Knight DA, Lenburg ME, Hogg JC,
268 Spira A. A gene expression signature of emphysema-related lung destruction and its
269 reversal by the tripeptide GHK. *Genome medicine* 2012; 4(8): 67.
- 270 4. Bhattacharya S, Srisuma S, Demeo DL, Shapiro SD, Bueno R, Silverman EK,
271 Reilly JJ, Mariani TJ. Molecular biomarkers for quantitative and discrete COPD
272 phenotypes. *American journal of respiratory cell and molecular biology* 2009; 40(3):
273 359-367.
- 274 5. Plank MW, Kaiko GE, Maltby S, Weaver J, Tay HL, Shen W, Wilson MS,
275 Durum SK, Foster PS. Th22 Cells Form a Distinct Th Lineage from Th17 Cells In
276 Vitro with Unique Transcriptional Properties and Tbet-Dependent Th1 Plasticity.
277 *Journal of immunology (Baltimore, Md : 1950)* 2017; 198(5): 2182-2190.

- 1
2
3
4 278 6. Fricker M GB, Mateer S, Jones B, Kim RY, Gellatly SL, Jarnicki AG, Powell N,
5 279 Oliver BG, Radford-Smith G, Talley NJ, Walker MM, Keely S, Hansbro PM. . Chronic
6 280 smoke exposure induces systemic hypoxia that drives intestinal dysfunction. . *JCI*
7 281 *insight* 2018(In Press).
- 8 282 7. Beckett EL, Stevens RL, Jarnicki AG, Kim RY, Hanish I, Hansbro NG, Deane
9 283 A, Keely S, Horvat JC, Yang M, Oliver BG, van Rooijen N, Inman MD, Adachi R,
10 284 Soberman RJ, Hamadi S, Wark PA, Foster PS, Hansbro PM. A new short-term
11 285 mouse model of chronic obstructive pulmonary disease identifies a role for mast cell
12 286 tryptase in pathogenesis. *The Journal of allergy and clinical immunology* 2013:
13 287 131(3): 752-762.
- 14 288 8. Haw TJ, Starkey MR, Pavlidis S, Fricker M, Arthurs AL, Mono Nair P, Liu G,
15 289 Hanish I, Kim RY, Foster PS, Horvat JC, Adcock IM, Hansbro PM. Toll-like receptor
16 290 2 and 4 have Opposing Roles in the Pathogenesis of Cigarette Smoke-induced
17 291 Chronic Obstructive Pulmonary Disease. *American journal of physiology Lung*
18 292 *cellular and molecular physiology* 2017: ajplung.00154.02017.
- 19 293 9. Haw TJ, Starkey MR, Nair PM, Pavlidis S, Liu G, Nguyen DH, Hsu AC,
20 294 Hanish I, Kim RY, Collison AM, Inman MD, Wark PA, Foster PS, Knight DA, Mattes
21 295 J, Yagita H, Adcock IM, Horvat JC, Hansbro PM. A pathogenic role for tumor
22 296 necrosis factor-related apoptosis-inducing ligand in chronic obstructive pulmonary
23 297 disease. *Mucosal immunology* 2016: 9(4): 859-872.
- 24 298 10. Hsu AC, Starkey MR, Hanish I, Parsons K, Haw TJ, Howland LJ, Barr I,
25 299 Mahony JB, Foster PS, Knight DA, Wark PA, Hansbro PM. Targeting PI3K-
26 300 p110alpha Suppresses Influenza Virus Infection in Chronic Obstructive Pulmonary
27 301 Disease. *American journal of respiratory and critical care medicine* 2015: 191(9):
28 302 1012-1023.
- 29 303 11. Hsu AC, Dua K, Starkey MR, Haw TJ, Nair PM, Nichol K, Zammit N, Grey ST,
30 304 Baines KJ, Foster PS, Hansbro PM, Wark PA. MicroRNA-125a and -b inhibit A20
31 305 and MAVS to promote inflammation and impair antiviral response in COPD. *JCI*
32 306 *insight* 2017: 2(7): e90443.
- 33 307 12. Liu G, Cooley MA, Jarnicki AG, Hsu AC, Nair PM, Haw TJ, Fricker M, Gellatly
34 308 SL, Kim RY, Inman MD, Tjin G, Wark PA, Walker MM, Horvat JC, Oliver BG,
35 309 Argraves WS, Knight DA, Burgess JK, Hansbro PM. Fibulin-1 regulates the
36 310 pathogenesis of tissue remodeling in respiratory diseases. *JCI insight* 2016: 1(9).
- 37 311 13. Hansbro PM, Hamilton MJ, Fricker M, Gellatly SL, Jarnicki AG, Zheng D, Frei
38 312 SM, Wong GW, Hamadi S, Zhou S, Foster PS, Krilis SA, Stevens RL. Importance of
39 313 mast cell Prss31/transmembrane tryptase/tryptase-gamma in lung function and
40 314 experimental chronic obstructive pulmonary disease and colitis. *The Journal of*
41 315 *biological chemistry* 2014: 289(26): 18214-18227.
- 42 316 14. Starkey MR, Nguyen DH, Essilfie AT, Kim RY, Hatchwell LM, Collison AM,
43 317 Yagita H, Foster PS, Horvat JC, Mattes J, Hansbro PM. Tumor necrosis factor-
44 318 related apoptosis-inducing ligand translates neonatal respiratory infection into
45 319 chronic lung disease. *Mucosal immunology* 2014: 7(3): 478-488.
- 46 320 15. Starkey MR, Essilfie AT, Horvat JC, Kim RY, Nguyen DH, Beagley KW,
47 321 Mattes J, Foster PS, Hansbro PM. Constitutive production of IL-13 promotes early-
48 322 life Chlamydia respiratory infection and allergic airway disease. *Mucosal immunology*
49 323 2013: 6(3): 569-579.
- 50 324 16. Kedzierski L, Tate MD, Hsu AC, Kolesnik TB, Linossi EM, Dagley L, Dong Z,
51 325 Freeman S, Infusini G, Starkey MR, Bird NL, Chatfield SM, Babon JJ, Huntington N,
52 326 Belz G, Webb A, Wark PA, Nicola NA, Xu J, Kedzierska K, Hansbro PM, Nicholson

- 1
2
3 327 SE. Suppressor of cytokine signaling (SOCS)5 ameliorates influenza infection via
4 328 inhibition of EGFR signaling. *eLife* 2017: 6.
- 5 329 17. Essilfie AT, Horvat JC, Kim RY, Mayall JR, Pinkerton JW, Beckett EL, Starkey
6 330 MR, Simpson JL, Foster PS, Gibson PG, Hansbro PM. Macrolide therapy
7 331 suppresses key features of experimental steroid-sensitive and steroid-insensitive
8 332 asthma. *Thorax* 2015: 70(5): 458-467.
- 9 333 18. Nair PM, Starkey MR, Haw TJ, Liu G, Horvat JC, Morris JC, Verrills NM, Clark
10 334 AR, Ammit AJ, Hansbro PM. Targeting PP2A and proteasome activity ameliorates
11 335 features of allergic airway disease in mice. *Allergy* 2017: 72(12): 1891-1903.
- 12 336 19. Horvat JC, Beagley KW, Wade MA, Preston JA, Hansbro NG, Hickey DK,
13 337 Kaiko GE, Gibson PG, Foster PS, Hansbro PM. Neonatal chlamydial infection
14 338 induces mixed T-cell responses that drive allergic airway disease. *American journal
15 339 of respiratory and critical care medicine* 2007: 176(6): 556-564.
- 16 340 20. Kim RY, Horvat JC, Pinkerton JW, Starkey MR, Essilfie AT, Mayall JR, Nair
17 341 PM, Hansbro NG, Jones B, Haw TJ, Sunkara KP, Nguyen TH, Jarnicki AG, Keely S,
18 342 Mattes J, Adcock IM, Foster PS, Hansbro PM. MicroRNA-21 drives severe, steroid-
19 343 insensitive experimental asthma by amplifying phosphoinositide 3-kinase-mediated
20 344 suppression of histone deacetylase 2. *The Journal of allergy and clinical immunology*
21 345 2017: 139(2): 519-532.
- 22 346 21. Kim RY, Pinkerton JW, Essilfie AT, Robertson AAB, Baines KJ, Brown AC,
23 347 Mayall JR, Ali MK, Starkey MR, Hansbro NG, Hirota JA, Wood LG, Simpson JL,
24 348 Knight DA, Wark PA, Gibson PG, O'Neill LAJ, Cooper MA, Horvat JC, Hansbro PM.
25 349 Role for NLRP3 Inflammasome-mediated, IL-1beta-Dependent Responses in
26 350 Severe, Steroid-Resistant Asthma. *American journal of respiratory and critical care
27 351 medicine* 2017: 196(3): 283-297.
- 28 352 22. Kirkham PA, Caramori G, Casolari P, Papi AA, Edwards M, Shamji B,
29 353 Triantaphyllopoulos K, Hussain F, Pinart M, Khan Y, Heinemann L, Stevens L,
30 354 Yeadon M, Barnes PJ, Chung KF, Adcock IM. Oxidative stress-induced antibodies to
31 355 carbonyl-modified protein correlate with severity of chronic obstructive pulmonary
32 356 disease. *American journal of respiratory and critical care medicine* 2011: 184(7):
33 357 796-802.
- 34 358 23. Marwick JA, Caramori G, Casolari P, Mazzone F, Kirkham PA, Adcock IM,
35 359 Chung KF, Papi A. A role for phosphoinositide 3-kinase delta in the impairment of
36 360 glucocorticoid responsiveness in patients with chronic obstructive pulmonary
37 361 disease. *The Journal of allergy and clinical immunology* 2010: 125(5): 1146-1153.
- 38 362 24. Caramori G, Adcock IM, Casolari P, Ito K, Jazrawi E, Tsaprouni L, Villetti G,
39 363 Civelli M, Carnini C, Chung KF, Barnes PJ, Papi A. Unbalanced oxidant-induced
40 364 DNA damage and repair in COPD: a link towards lung cancer. *Thorax* 2011: 66(6):
41 365 521-527.
- 42 366 25. Tam A, Hughes M, McNagny KM, Obeidat M, Hackett TL, Leung JM,
43 367 Shaipanich T, Dorscheid DR, Singhera GK, Yang CWT, Pare PD, Hogg JC, Nickle
44 368 D, Sin DD. Hedgehog signaling in the airway epithelium of patients with chronic
45 369 obstructive pulmonary disease. *Scientific reports* 2019: 9(1): 3353.

370

371

372

1
2
3 **373 Supplementary figure legends**
4

5
6 **374 Supplementary Figure 1: Gating strategy for lung immune cell subsets. (a)**
7

8 **375 CD4⁺ T cells, (b) $\gamma\delta$ T cells and NKT cells and (c) ILC3.**
9

10
11
12 **376**

13
14 **377 Supplementary Figure 2: IL-22 and receptor mRNA in human peripheral lung**

15 **378 tissue is unchanged in mild emphysema.** Microarray data from peripheral lung

16 **379 tissue of patients with mild emphysema (Accession: GSE8581). (a) IL-22, (b) IL-**

17 **380 22RA1, (c) IL-22RA1 and (d) IL-10RB.** Data are represented as log₂ intensity robust

18 **381 multi-array average signals.**
19
20
21
22
23
24
25
26
27 **382**

28
29 **383 Supplementary Figure 3: No correlation between smoking pack-years and IL-**

30 **384 22 or receptor expression. (a) IL-22, (b) IL-22RA1, (c) IL-22RA2**
31
32
33
34
35 **385**
36
37

38 **386 Supplementary Figure 4: No change in IL-22 or receptors in bronchial**

39 **387 brushings in lung cancer.** Microarray data from bronchial brushings in lung cancer

40 **388 (Accession: GSE4115). (a) IL-22, (b) IL-22RA1, (c) IL-10RB.** Data are represented

41 **389 as log₂ intensity robust multi-array average signals.**
42
43
44
45
46
47
48 **390**
49

50 **391 Supplementary Figure 5: No change in IL-22 or receptors in lung tissue in lung**

51 **392 cancer.** Microarray data from lung tissue in lung cancer (Accession: GSE1650). **(a)**

52 **393 IL-22, (b) IL-22RA1, (c) IL-10RB.** Data are represented as log₂ intensity robust multi-

53 **394 array average signals.**
54
55
56
57
58
59
60

1
2
3 395 **Supplementary figure 6: Representative images of IL-22 and IL-22 receptor**
4
5 396 **staining in human lung tissue.** The four panels are showing the representative
6
7 397 images of IL-22 (upper panel), IL-22RA1 (upper middle panel), IL-22RA2 (lower
8
9 398 middle panel) and IL-10RB (lower panel) immunohistochemical staining in human
10
11 399 peripheral lung tissue. **(a and d)** represent age- and smoke history-matched control
12
13 400 smokers with normal lung function and **(b and e)** represent mild-to-moderate stable
14
15 401 COPD. Upper lane images show the bronchiolar epithelium whereas lower lanes the
16
17 402 alveolar macrophages. Representative images of positive control tissues (tonsils for
18
19 403 IL-22, IL-22RA1 and IL-10RB), normal kidney for IL-22RA2 (kindly provided
20
21 404 respectively by Prof Stefano Pelucchi and Prof Carmelita Di Gregorio) were stained
22
23 405 with primary antibody **(c)** or with nonspecific immunoglobulin (Ig)G (negative control,
24
25 406 **f**). Total magnification: 1000x **(a, b, d, e;** bar = 20 μm) or 200x **(c, f;** bar = 100 μm).

31
32 407
33
34 408 **Supplementary figure 7: Increased IL-22RA1 protein intensity in the airway**
35
36 409 **epithelium of smokers with COPD. (a) IL-22RA1 protein intensity per micrometre**
37
38 410 **(μm) of basement membrane (BM) in non-smokers, healthy smokers without COPD**
39
40 411 **and COPD with or without current smoking separated into GOLD stage 2 and GOLD**
41
42 412 **stage 3-4. (b) IL-22RA1 intensity in airway epithelium of non-smokers vs. smokers**
43
44 413 **with COPD. (c) Representative images of IL-22RA1 positive staining, with red**
45
46 414 **staining in the airway epithelial cells indicating IL-22RA1 positive staining.**

51 415
52
53
54 416 **Supplementary figure 86: IL-22 protein levels are unaltered in the lungs of mice**
55
56 417 **exposed to CS for 1 week.** Wild-type (WT) C57BL/6 mice were exposed to normal
57
58 418 air or CS for 1 week. IL-22 protein levels in lung homogenates were assessed by
59
60

1
2
3 419 ELISA. Data are presented as mean \pm SEM, n = 6, with another independent
4
5 420 experiment showing similar results. Two-tailed Mann-Whitney t-test was used to
6
7 421 analyse differences between two groups.
8
9

10 422

11
12
13 **423 Supplementary figure 97: Representative images of IL-22RA1 and IL-22RA2**

14
15 424 **protein in mouse lung tissue sections.** Wild-type (WT) C57BL/6 mice were

16
17 425 exposed to normal air or CS for 8 weeks. Representative images of negative control

18
19 426 (top row), IL-22RA1 and IL-22RA2 staining in mouse lung tissue sections from

20
21 427 normal air- (left) and CS-exposed (right) mice.
22
23
24

25 428

26
27
28 **429 Supplementary figure 108: IL-17A, MPO and neutrophil elastase protein levels**

29
30 430 **are increased in experimental COPD, but not in the absence of IL-22.** Wild-type

31
32 431 (WT) and IL-22-deficient (*Il22^{-/-}*) C57BL/6 mice were exposed to normal air or CS for

33
34 432 8 weeks to induce experimental COPD. (a) IL-17A, (b) MPO and (c) neutrophil

35
36 433 elastase protein levels in lung homogenates. Data are presented as mean \pm SEM, n

37
38 434 = 6, with another independent experiment showing similar results. The one-way

39
40 435 analysis of variance with Bonferroni post-test analysed differences between 3 or

41
42 436 more groups, whereby * = $p < 0.05$ compared to normal air-exposed controls. ns = not

43
44 437 significant.
45
46
47
48

49 438

50
51
52 **439 Supplementary Figure 119: CS induced non-significant reductions in tissue**

53
54 440 **elastance that was not different in *Il22^{-/-}* mice.** Wild-type (WT) and IL-22-deficient

55
56 441 (*Il22^{-/-}*) C57BL/6 mice were exposed to normal air or CS for 8 weeks to induce

57
58 442 experimental COPD. Lung function was assessed in terms of tissue elastance. Data
59
60

1
2
3 443 are presented as mean \pm SEM, n = 6, with another independent experiment showing
4
5 444 similar results. The one-way analysis of variance with Bonferroni post-test analysed
6
7 445 differences between 3 or more groups. ns = not significant.
8
9
10
11
12
13
14
15
16
17
18
19
20
21
22
23
24
25
26
27
28
29
30
31
32
33
34
35
36
37
38
39
40
41
42
43
44
45
46
47
48
49
50
51
52
53
54
55
56
57
58
59
60

1
2
3
4
5
6
7
8
9
10
11
12
13
14
15
16
17
18
19
20
21
22
23
24
25
26
27
28
29
30
31
32
33
34
35
36
37
38
39
40
41
42
43
44
45
46
47
48
49
50
51
52
53
54
55
56
57
58
59
60

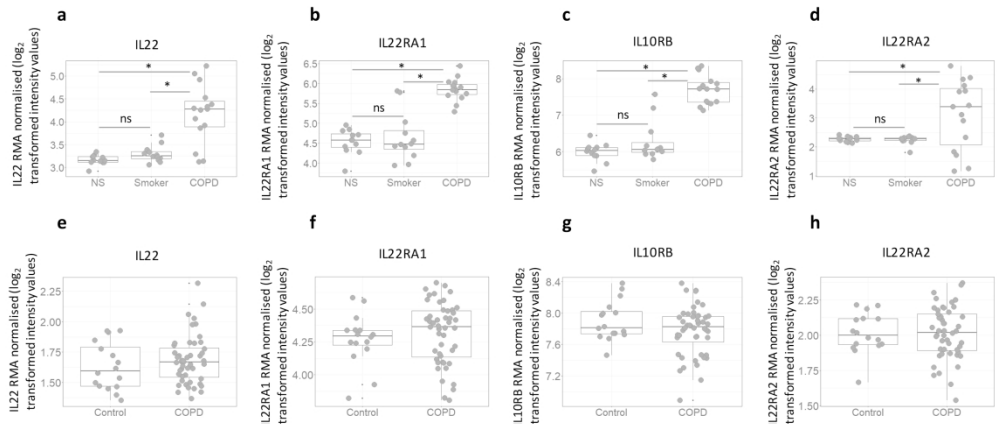


Figure 1

269x119mm (300 x 300 DPI)

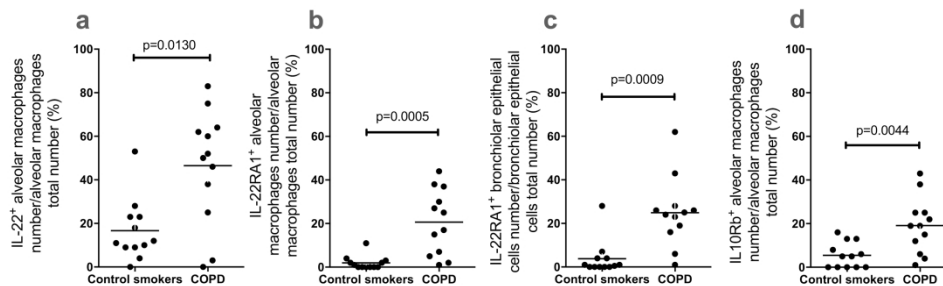


Figure 2

272x81mm (300 x 300 DPI)

1
2
3
4
5
6
7
8
9
10
11
12
13
14
15
16
17
18
19
20
21
22
23
24
25
26
27
28
29
30
31
32
33
34
35
36
37
38
39
40
41
42
43
44
45
46
47
48
49
50
51
52
53
54
55
56
57
58
59
60

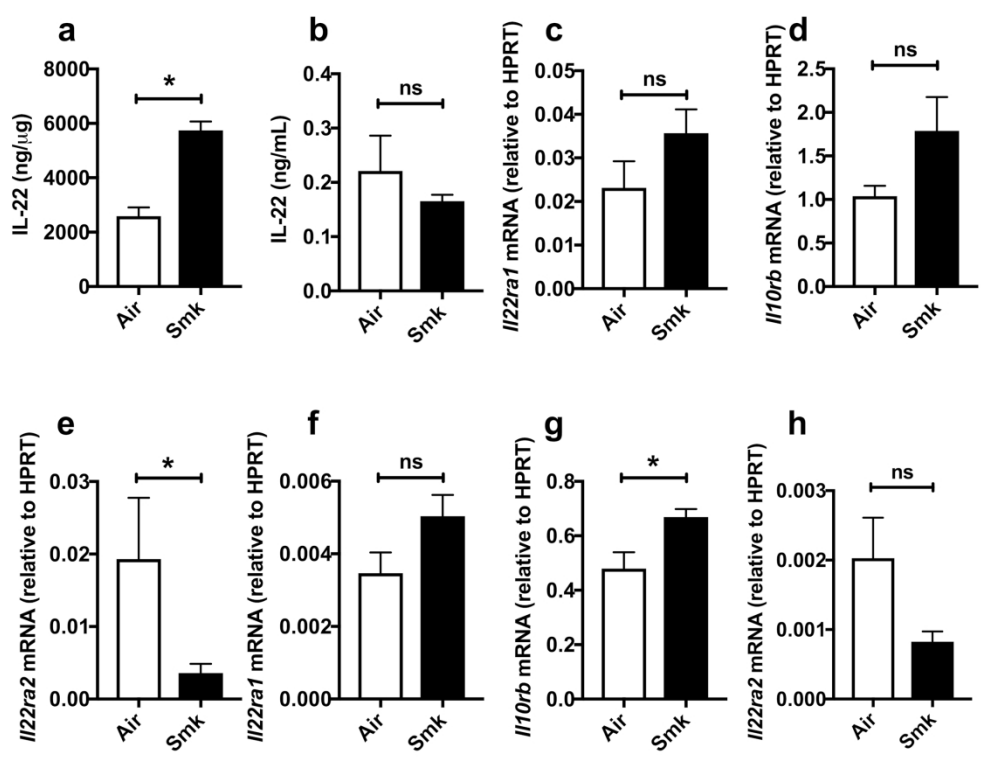


Figure 3

209x161mm (300 x 300 DPI)

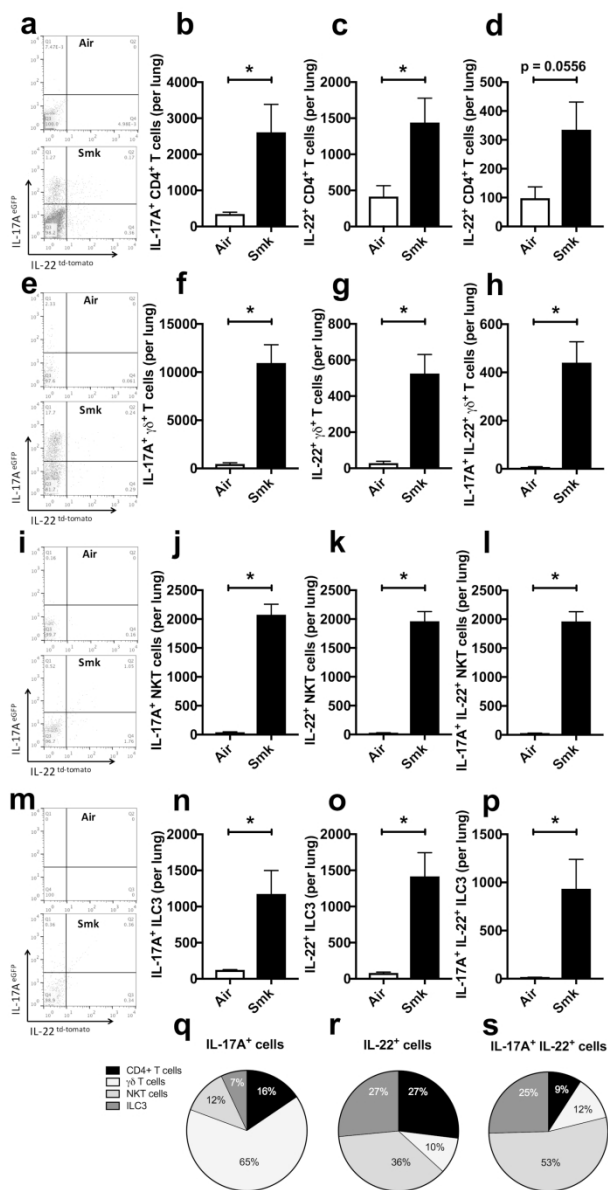


Figure 4

140x273mm (300 x 300 DPI)

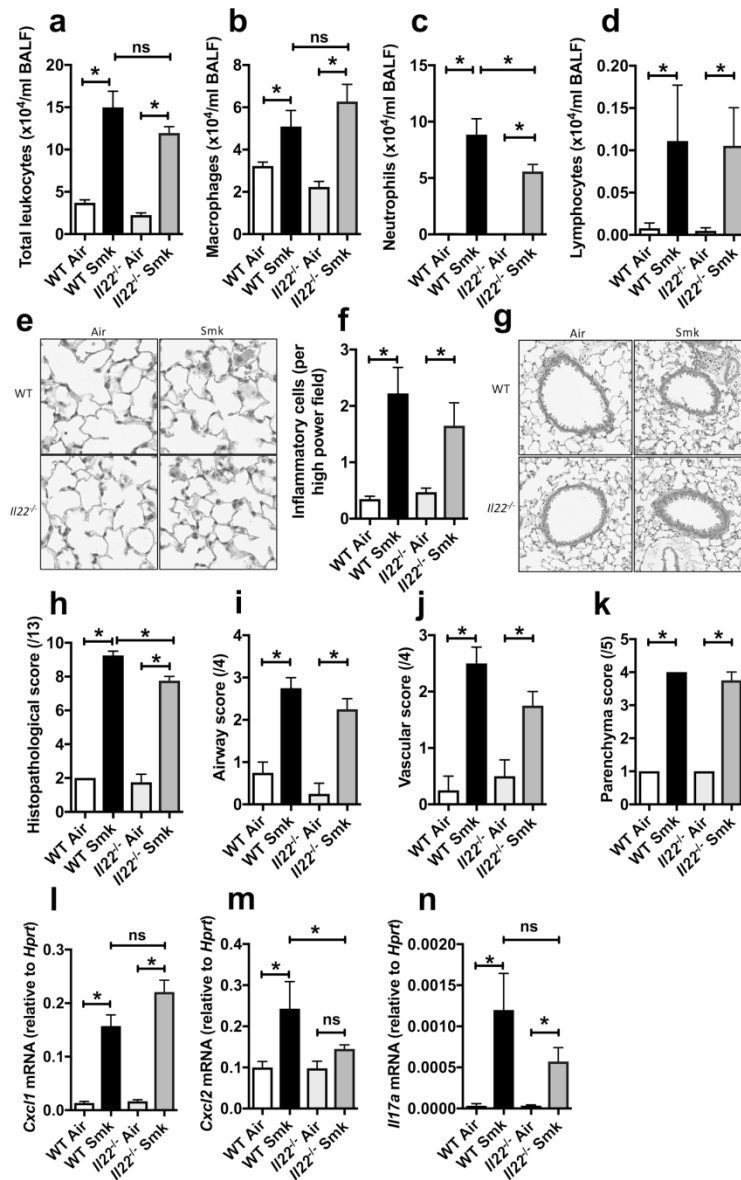


Figure 5

163x258mm (300 x 300 DPI)

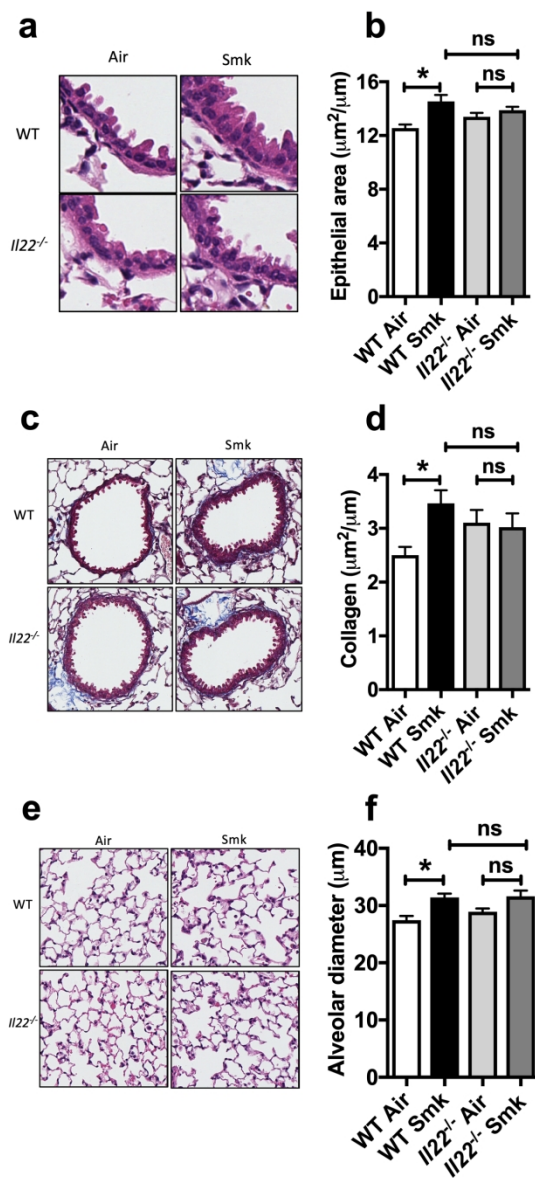


Figure 6

109x235mm (300 x 300 DPI)

1
2
3
4
5
6
7
8
9
10
11
12
13
14
15
16
17
18
19
20
21
22
23
24
25
26
27
28
29
30
31
32
33
34
35
36
37
38
39
40
41
42
43
44
45
46
47
48
49
50
51
52
53
54
55
56
57
58
59
60

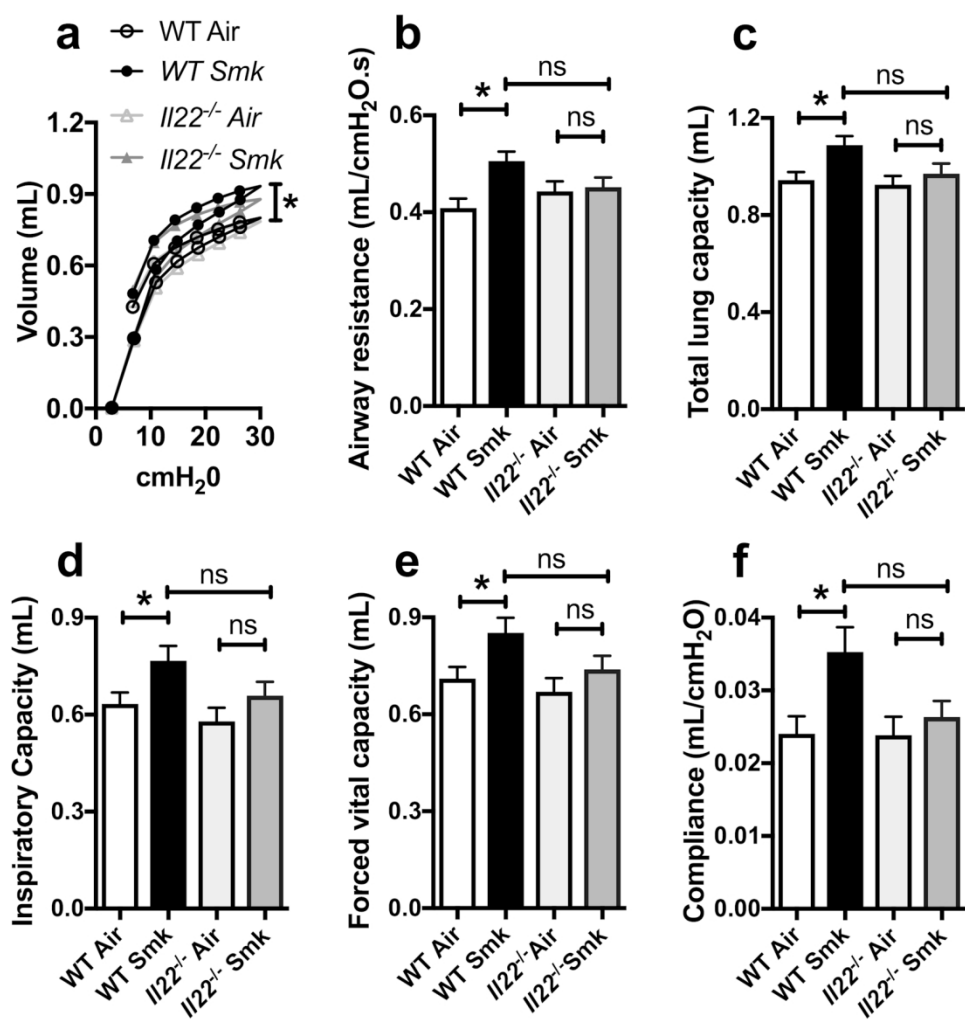
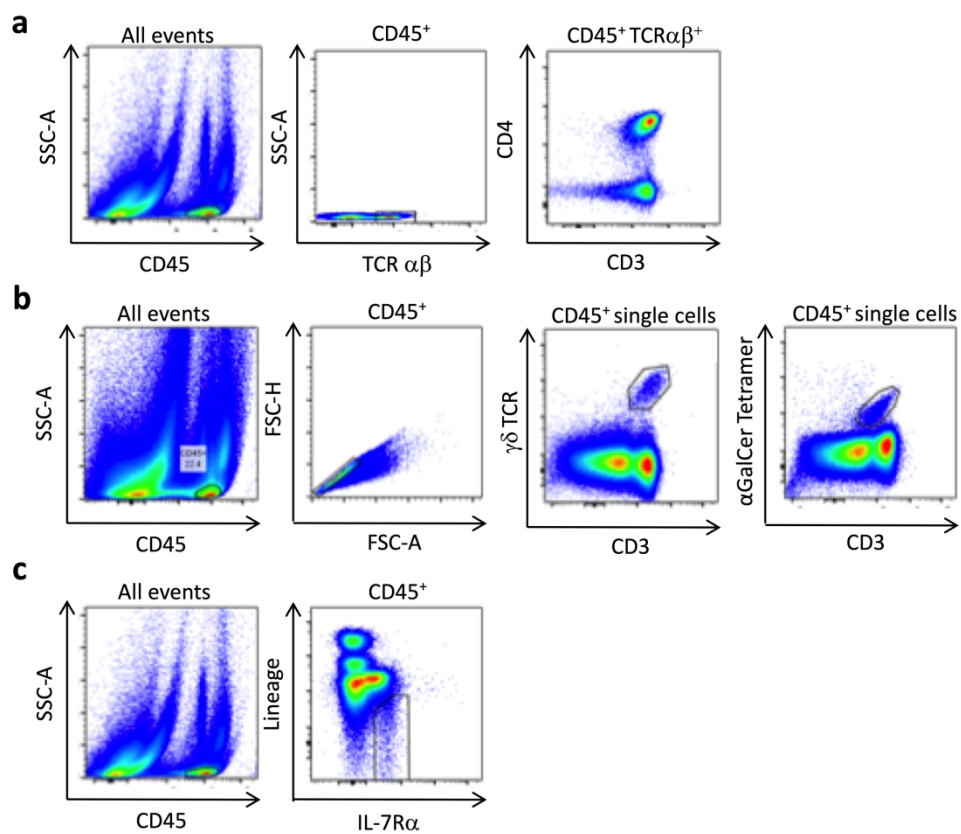


Figure 7

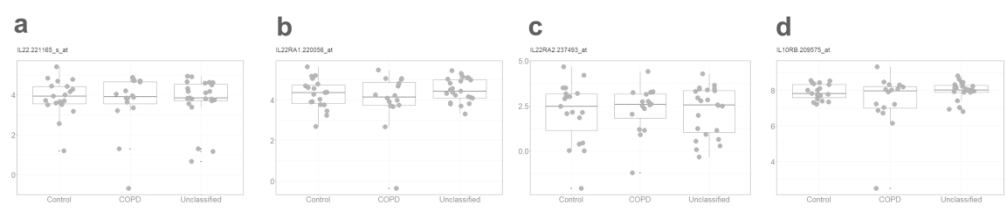
149x157mm (300 x 300 DPI)



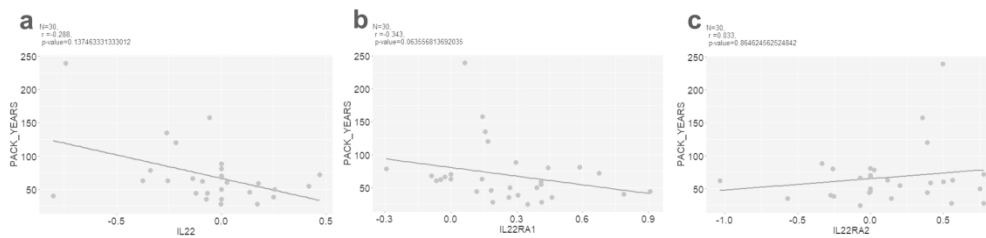
221x191mm (300 x 300 DPI)

1
2
3
4
5
6
7
8
9
10
11
12
13
14
15
16
17
18
19
20
21
22
23
24
25
26
27
28
29
30
31
32
33
34
35
36
37
38
39
40
41
42
43
44
45
46
47
48
49
50
51
52
53
54
55
56
57
58
59
60

1
2
3
4
5
6
7
8
9
10
11
12
13
14
15
16
17
18
19
20
21
22
23
24
25
26
27
28
29
30
31
32
33
34
35
36
37
38
39
40
41
42
43
44
45
46
47
48
49
50
51
52
53
54
55
56
57
58
59
60



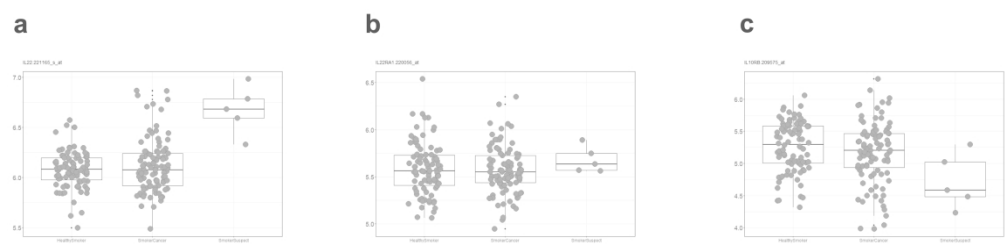
265x54mm (300 x 300 DPI)



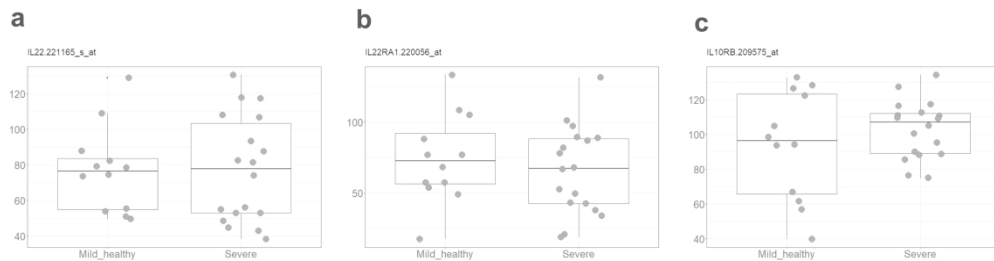
270x65mm (300 x 300 DPI)

1
2
3
4
5
6
7
8
9
10
11
12
13
14
15
16
17
18
19
20
21
22
23
24
25
26
27
28
29
30
31
32
33
34
35
36
37
38
39
40
41
42
43
44
45
46
47
48
49
50
51
52
53
54
55
56
57
58
59
60

1
2
3
4
5
6
7
8
9
10
11
12
13
14
15
16
17
18
19
20
21
22
23
24
25
26
27
28
29
30
31
32
33
34
35
36
37
38
39
40
41
42
43
44
45
46
47
48
49
50
51
52
53
54
55
56
57
58
59
60



270x65mm (300 x 300 DPI)

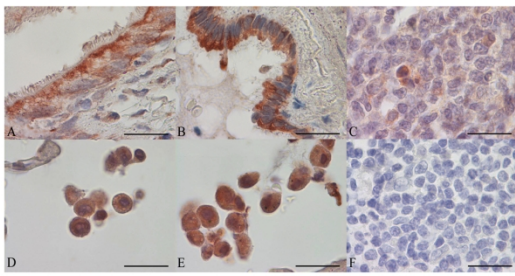


267x70mm (300 x 300 DPI)

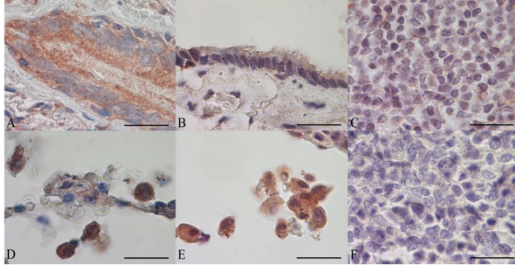
1
2
3
4
5
6
7
8
9
10
11
12
13
14
15
16
17
18
19
20
21
22
23
24
25
26
27
28
29
30
31
32
33
34
35
36
37
38
39
40
41
42
43
44
45
46
47
48
49
50
51
52
53
54
55
56
57
58
59
60

1
2
3
4
5
6
7
8
9
10
11
12
13
14
15
16
17
18
19
20
21
22
23
24
25
26
27
28
29
30
31
32
33
34
35
36
37
38
39
40
41
42
43
44
45
46
47
48
49
50
51
52
53
54
55
56
57
58
59
60

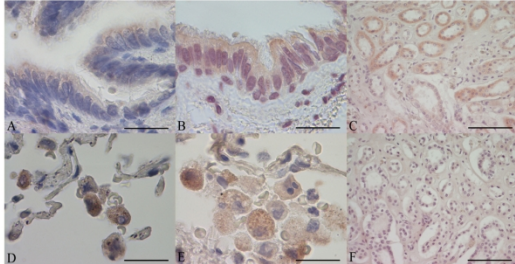
IL-22



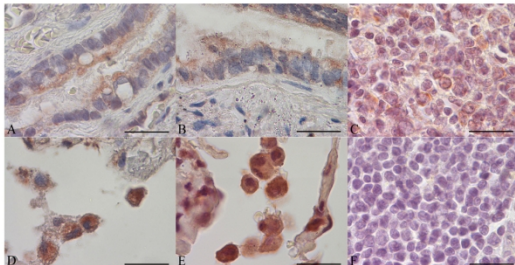
IL-22RA1



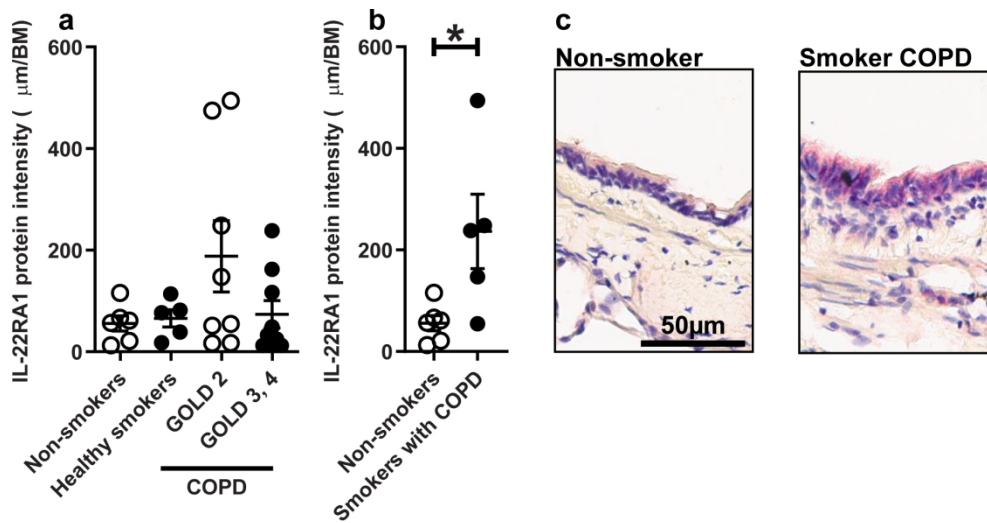
IL-22RA2



IL-10RB

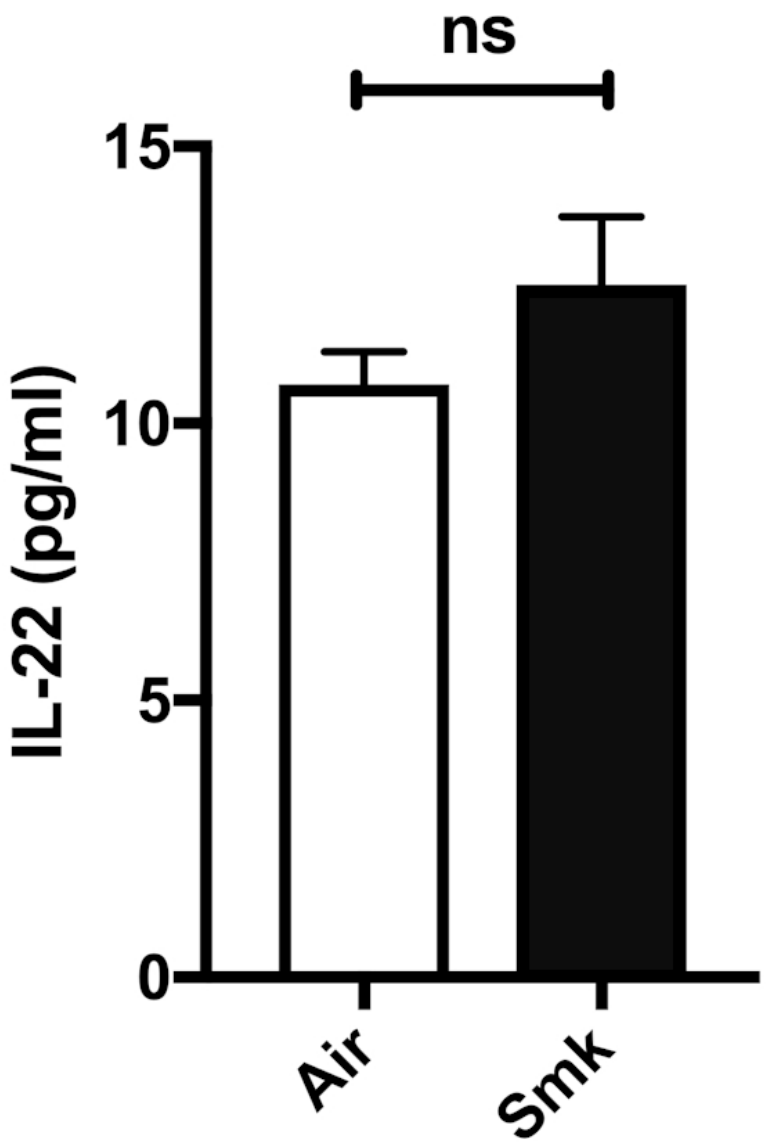


116x267mm (300 x 300 DPI)



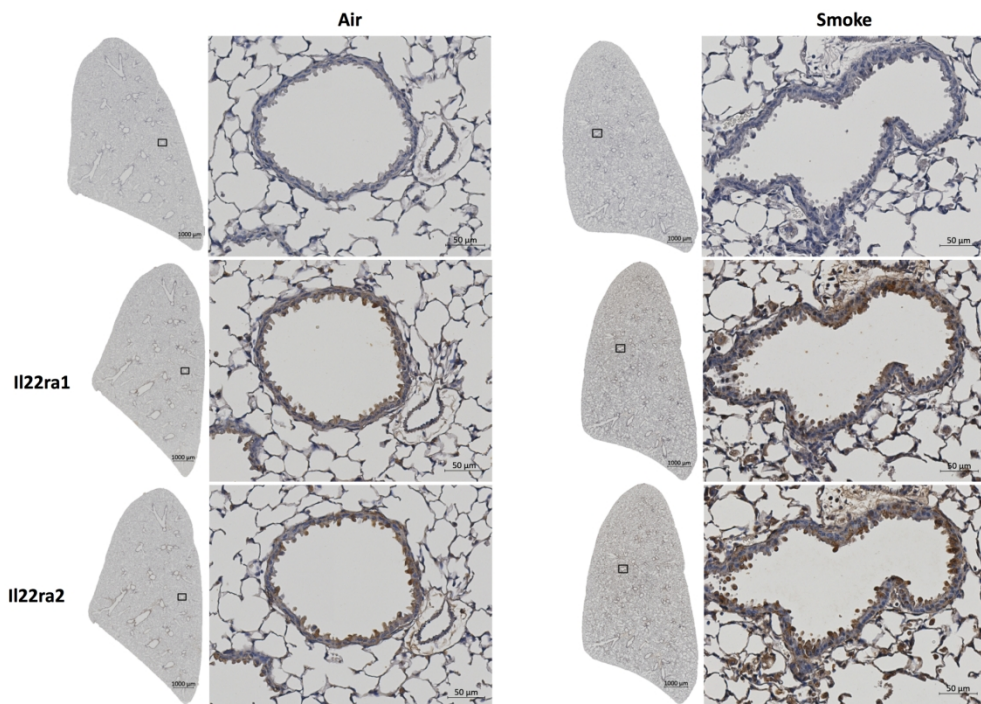
1
2
3
4
5
6
7
8
9
10
11
12
13
14
15
16
17
18
19
20
21
22
23
24
25
26
27
28
29
30
31
32
33
34
35
36
37
38
39
40
41
42
43
44
45
46
47
48
49
50
51
52
53
54
55
56
57
58
59
60

1
2
3
4
5
6
7
8
9
10
11
12
13
14
15
16
17
18
19
20
21
22
23
24
25
26
27
28
29
30
31
32
33
34
35
36
37
38
39
40
41
42
43
44
45
46
47
48
49
50
51
52
53
54
55
56
57
58
59
60

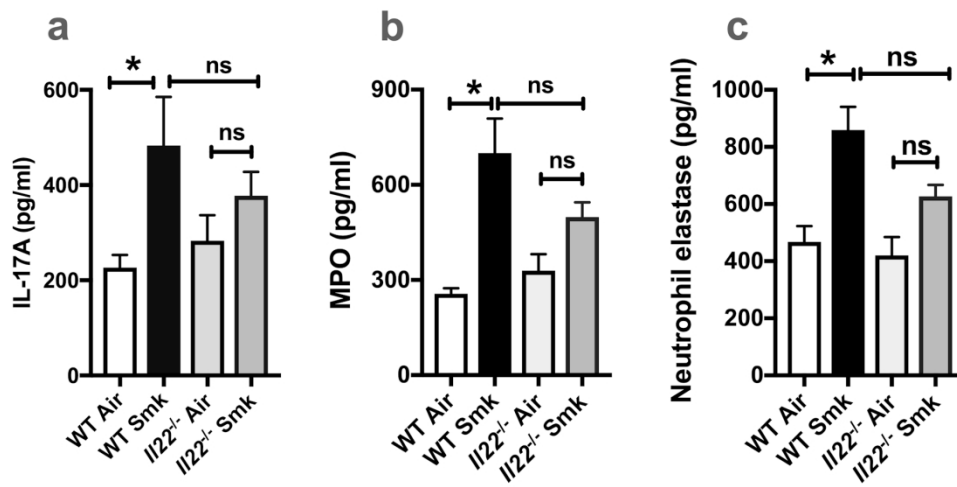


50x73mm (300 x 300 DPI)

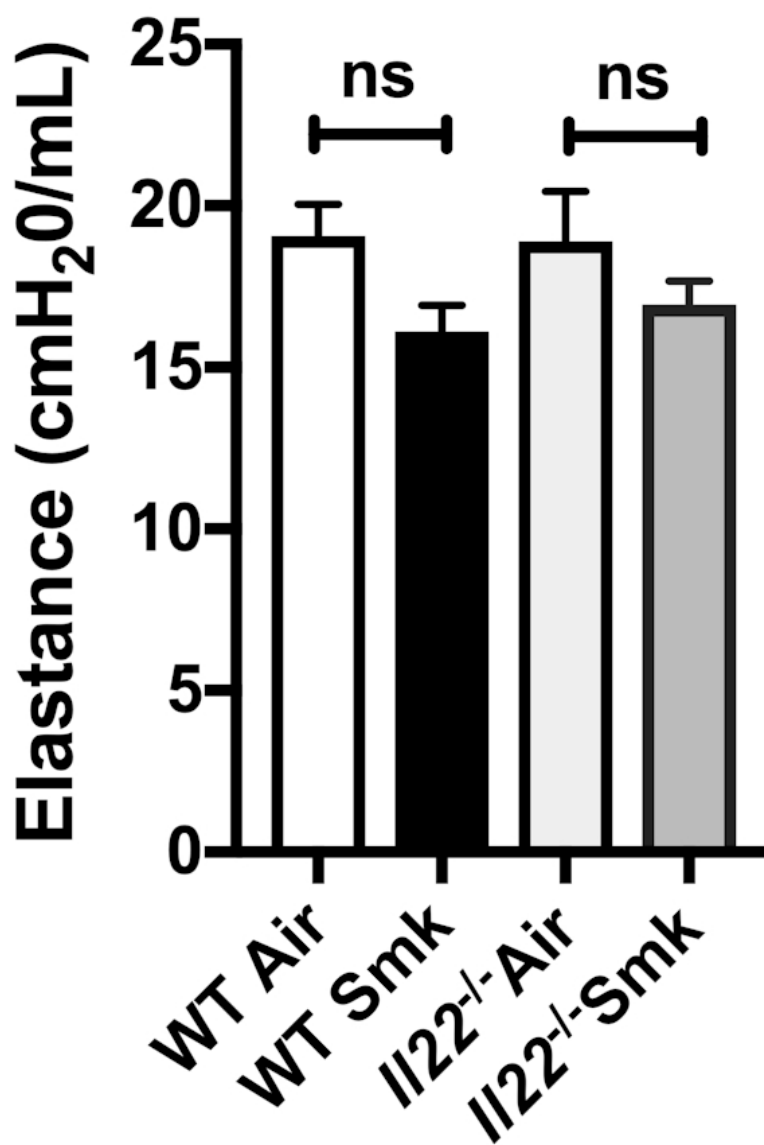
1
2
3
4
5
6
7
8
9
10
11
12
13
14
15
16
17
18
19
20
21
22
23
24
25
26
27
28
29
30
31
32
33
34
35
36
37
38
39
40
41
42
43
44
45
46
47
48
49
50
51
52
53
54
55
56
57
58
59
60



176x125mm (300 x 300 DPI)



170x88mm (300 x 300 DPI)



52x75mm (300 x 300 DPI)